UCRL-JC-129618
PREPRINT

Linear Induction Accelerator Requirements for Ion Fast Ignition

G. Logan

This paper was prepared for submittal to the
15th International Workshop on High Energy Density in Matter
Hirschegg, Austria
February 2-6, 1998

January 26, 1998

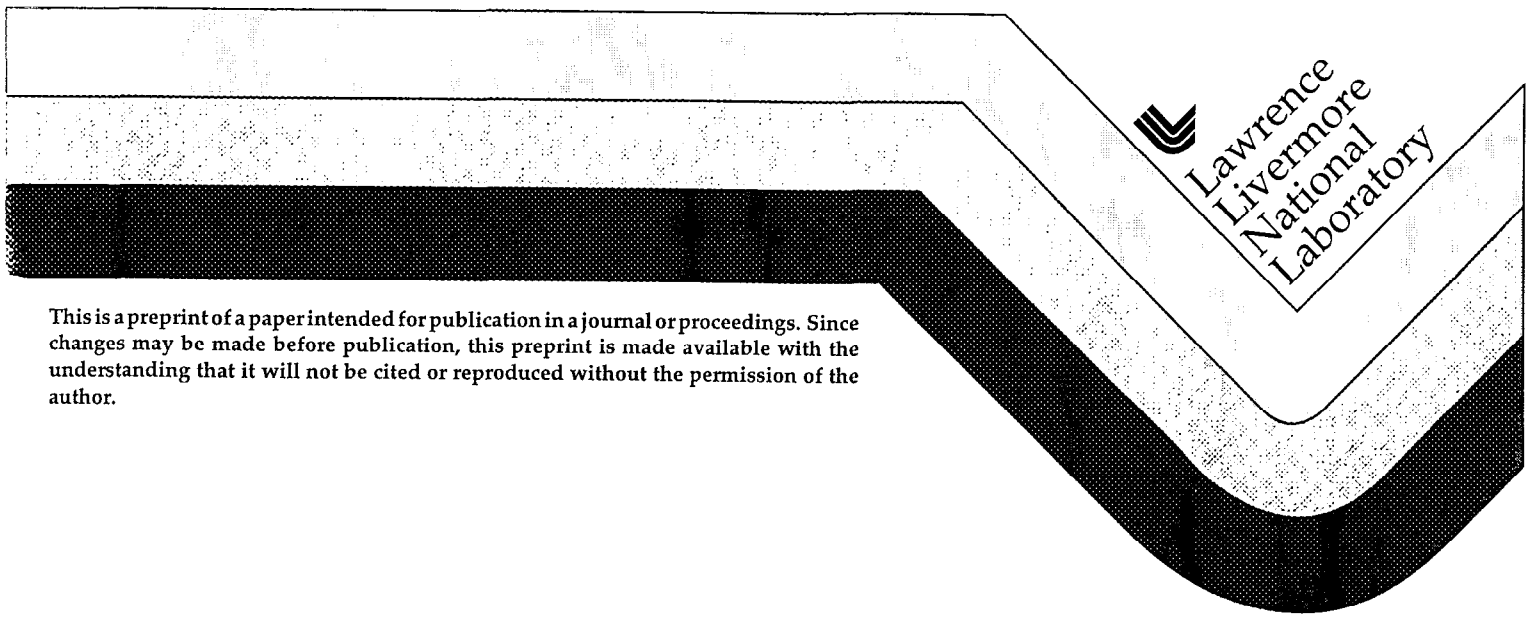

Linear induction accelerator requirements for ion fast ignition

Grant Logan
Lawrence Livermore National Laboratory*

15th international workshop on "High Energy Density in Matter"
Hirschegg, Austria
(sponsored by GSI and Karlsuhe Labs, Germany)
Feb. 2-7, 1998

* Work performed under the auspices of the U.S. Department of Energy by the Lawrence Livermore National Laboratory under contract number W-7405-ENG-48

MathCAD MEMO
Date: January 8, 1997
To: John Lindl, Alex Friedman, Roger Bangerter, George Caporaso, Hugh Kirbie, Debbie Callahan, John Perkins, Max Tabak, Ed Lee, Andy Faltens
From: Grant Logan

Subject: **Linear induction accelerator requirements for ion fast ignition**

Contents:

I. Introduction

Fast ignition (fast heating of DT cores *after* compression) reduces driver energy (by 10 X or more) by reducing the implosion velocity and energy for a given fuel compression ratio. For any type of driver that can deliver the ignition energy fast enough, fast ignition increases the target gain compared to targets using fast implosions for central ignition, as long as the energy to heat the core after compression is comparable to or less than the slow compression energy, and as long as the coupling efficiency of the fast ignitor beam to heat the core is comparable to the overall efficiency of compressing the core (in terms of beam energy-to-DT-efficiency). Ion driven fast ignition, compared to laser-driven fast ignition, has the advantage of direct (dE/dx) deposition of beam energy to the DT, eliminating inefficiencies for conversion into hot electrons, and direct ion heating also has a more favorable deposition profile with the Bragg-peak near the end of an ion range chosen to be deep inside a compressed DT core.

While Petawatt laser experiments at LLNL have demonstrated adequate light-to-hot-electron conversion efficiency, it is not yet known if light and hot electrons can channel deeply enough to heat a small portion of a 1000xLD compressed DT core to ignition. On the other hand, lasers with chirped-pulse amplification giving thousand-fold pulse compressions have been demonstrated to produce the short pulses, small focal spots and Petawatt peak powers approaching those required for fast ignition, whereas ion accelerators that can produce sufficient beam quality for similar compression ratios and focal spot sizes of ion bunches have not yet been demonstrated, where an imposed coherent velocity tilt plays the analogous role for beam compression as does frequency chirp with lasers.

Accordingly, it is the driver technology, not the target coupling physics, that poses the main challenge to ion-driven fast ignition. As the mainline HIF program is concentrating on induction linacs, the purpose of this memo is to explore possible new features and characteristic parameters that induction linacs would need to meet the stringent requirements for beam quality and compression (sufficiently low longitudinal and transverse thermal spread) for ion driven fast ignition. Separately, Ed Lee at LBNL is looking at heavy-ion synchrotrons to meet similar fast ignition requirements. Parameters relating to cost (e.g, total beam-line length and transport quads, total core volt-seconds and power switching) have to be considered in addition to meeting the challenging beam quality requirements for fast ignition compared to conventional HIF. The aim of this preliminary study is to motivate, after critical debate, taking a next step to do more detailed designs, particle simulations, and experimental tests of the most critical accelerator elements and focusing optics, to further assess the feasibility of ion-driven fast ignition. I wish to acknowledge useful discussions with George Caporaso and Hugh Kirbie on accelerator ideas, with John Barnard on formulas, and with Max Tabak and Debbie Callahan on fast ignition targets.

Target requirements

Debbie Callahan and John Perkins are currently developing a "target road map" in ρ versus ρr space for ion-driven fast ignition, to give accelerators designers a way to optimize choices of accelerator and target parameters together. When that road map is finished, the "best" accelerator (either linac or synchrotron) can be optimized. However, either type of accelerator will likely need some new design features to meet stringent fast ignition pulse requirements that will be more challenging than conventional HIF anywhere in the ρ vs ρr space. To explore what new features might be required for induction linacs, this memo considers a specific linac example to meet the following requirements of a recent 2-D target burn calculation by Debbie Callahan for ion-driven fast ignition (just the ignition part- the compression beam system, (easier), can be added later) : (1) a Gaussian ignitor ion beam radius equal to the compressed core radius [beam spot radius r_s = DT compressed core radius= 156 μm], (2) Total incident ignitor beam energy =300 kJ. (3) an ion range R equal to the compressed core = ρr_c = 4 g/cm^2 , and (4) a final ion pulse duration $\tau_f = 0.3\ r_c / 10^8 = 50$ ps.

This example target with a rather low fuel compression ratio (1000x) is chosen to promote the possibility that such a target could be both compressed and ignited by ion beams coming from a single direction, simplifiying the chamber design. For beam energy required for fuel compression, Max Tabak estimates 12 % overall efficiency at an adiabat parameter α = 2, assuming a "close-coupled" hohlraum with a modest convergence ratio ~10 to15 sufficient for ρ_f = 256 g/cm^3. With these assumptions, the ion beam energy for compression is about 650 kJ. The fusion yield in Debbies 2-D burn calculation was ~ 370 MJ, so that the target gain would be G= 370/0.9 = 410, more than sufficient for accelerators with efficiencies as low as 5 %. Earlier, Max Tabak had calculated a minimum energy for ion ignition to be 50 kJ, but that had to be delivered in 50 ps within a 30 μm radius spot. Since the greatest challenge will be getting sufficient beam quality and pulse compression to achieve a much smaller spot size and shorter pulse length compared to conventional HIF, this memo adopts the larger ignition beam energy case as a compromise between target gain and accelerator difficulty.

Summary of findings (from this preliminary study)

(1) Using a consistent model for contributions of both transverse and longitudinal velocity spread to focal spots, this study finds that 156 μm spot size and 50 ps pulse length can be achieved for a several ion masses and charge states, with high charge states and heavy ions favored over lower mass q=1 ions having both the same charge to mass ratio and ion range, for fast ignition.

(2) Despite high ion kinetic energy for fast ignition at ρr = 4 g/cm^2 , partial neutralization of high-q beam space charge is still required in the target chamber, but to a lesser degree than already required for current HIF "conventional" targets. PIC calculations of beam neutralization for q = 1 ions (1995 HIF Symposium paper by Callahan) and for high-q ions (1997 Symposium paper by Callahan and Logan), suggest ways to make space charge negligible for focusing ions @ 4 g/cm^2.

(3) Velocity tilts required for drift compression of 4 g/cm^2 ions cannot be removed at final focus by beam space charge with reasonable lengths and peak beam potentials for fast ignition cases. This necessitates time-varying correction for chromatic aberration such as by a fast-rising e-beam injected along a cone co-axial with the ion beam (providing ~1 % focusing field ramps in ~1 ns).

(4) Achieving 50 ps pulses on target requires starting acceleration with much shorter pulses << 10 μs, and compressing them as much as possible during acceleration. This leads to much shorter induction pulses (< 50 ns) at the higher energy end of the accelerator, probably requiring either dielectric-wall radial transmission lines [DWA-type (Caporaso/Sampayan)] or use of ferrite cores and fast FET switching with at least one or two stages of magnetic pulse compression using non-linear saturation of ferrite.

II. Model for beam velocity spread, pulse compression, and final focus

$M_p := 1.67 \cdot 10^{-27}$ (kg) the mass of a proton,

$e := 1.6 \cdot 10^{-19}$ (C) electron charge,

$c := 3 \cdot 10^{8}$ (m/s) the speed of light,

$I_o := 3.1 \cdot 10^{7}$ (Amps) -constant in beam perveance)

$\varepsilon_o := 8.85 \cdot 10^{-12}$ Vacuum permittivity (Farads/m),

$\mu_o := 4 \cdot \pi \cdot 10^{-7}$ Vacuum permeability (Henrys/m)

$\gamma(T,A) := 1 + \frac{e \cdot T}{A \cdot M_p \cdot c^2}$ the relativistic gamma factor, with T the kinetic energy in eV, A the atomic mass number

$\beta(T,A) := \sqrt{1 - \gamma(T,A)^{-2}}$ the ion velocity normalized to c.

Neutralization of beam space charge

Consider examples with Xenon ions @ $T_f := 40 \cdot 10^{9}$ (eV), for 4 g/cm^2 range, $A := 131$

Total ignitor beam energy on target $E_{ig} := 300 \cdot 10^{3}$ (J), [Callahan's 2-D example],

delivered by $N_b := 50$ beams in $\tau_f := 50 \cdot 10^{-12}$ (s), [Callahan's 2-D example].

within a target spot radius $r_s := 156 \cdot 10^{-6}$ (m), [Callahan's 2-D example].

The peak current per beam <u>on target</u> is $I_f(E_{ig}, T_f, A, q, N_b) := \frac{q \cdot E_{ig}}{T_f \cdot N_b \cdot \tau_f}$ (Amps), Eq. 1

$I_f(E_{ig}, T_f, A, 1, N_b) = 3 \cdot 10^{3}$ (A), for q=1, and

$I_f(E_{ig}, T_f, A, 26, N_b) = 7.8 \cdot 10^{4}$ (A) for q=26.

Because of appreciable beam drift compression over a $L_f := 5$ (m) focal length to the target, the beam current is 3.5 x lower, and pulse duration 3.5 x longer <u>at the final focus lens</u> (see pg.11).

Assuming a beam radius $a_f := 0.05$ (m), gives a nominal focusing angle $\theta_f := a_f \cdot L_f^{-1}$

of $\theta_f = 0.01$ (rad).

The dimensionless beam perveance required to meet the required spot size at 5 meters is then

$$K(\theta_f, a_f, r_s) := \theta_f^2 \cdot \left(2 \cdot \ln\left(\frac{a_f}{r_s}\right)\right)^{-1} \qquad K(\theta_f, a_f, r_s) = 8.666 \cdot 10^{-6} \qquad \text{Eq. 2}$$

The percentage factor by which the beam space charge must be reduced to meet this perveance requirement is given by $\%F_{sc}$:

$$F(\theta_f, a_f, r_s, T_f, q, A, I_b) := \frac{I_o}{I_b} \cdot K(\theta_f, a_f, r_s) \cdot \left(\beta(T_f, A) \cdot \gamma(T_f, A)\right)^3 \cdot \frac{A}{2 \cdot q}$$

$$\%F_{sc}(\theta_f, a_f, r_s, T_f, q, A, I_b) := \text{if}\left(F(\theta_f, a_f, r_s, T_f, q, A, I_b) > 1, 0, \frac{1 - F(\theta_f, a_f, r_s, T_f, q, A, I_b)}{0.01}\right)$$

Eq. 3

For our two charge states of Xenon, the required % space charge neutralization factors are

$\%F_{sc}\left(\theta_f, a_f, r_s, T_f, 1, A, I_f\left(E_{ig}, T_f, A, 1, N_b\right)\right) = 0$ (%) for q=1, and

$\%F_{sc}\left(\theta_f, a_f, r_s, T_f, 26, A, I_f\left(E_{ig}, T_f, A, 26, N_b\right)\right) = 99.4$ (%), for q = 26.

Since we must allow for some emittance and aberration contributions to the spot size, we will actually need some neutralization at q=1, and better than 99.4%, say, 99.6 % or more, for the q=26 example. Using Bruce Langdon's BICrz 2-D PIC code, Callahan has shown earlier that a low density plasma (0.5 % ionization of the Flibe vapor in the chamber) can provide >90% neutralization of 7.5 kA q =1 Cesium beams (1995 Symposium), and in a later paper (1997 Heidelberg Symposium), we showed that a cold electron source at the beam entrance to the chamber (such as a plasma lens might provide) could neutralize better than pre-formed plasma in the chamber, providing neutralization of 28 kA, q = 8 Xenon beams to within 99.8 %, 3 x better than the 99.4% estimated above for the q =26 Xenon case. More space charge neutralization calculations need to be done to check these conclusions for fast ignition, but to simplify the following analysis, we will assume that beam space-charge neutralization can be accomplished well enough (especially using the cold electron source method) that the effects of space charge on target spot size can be neglected compared to the effects of transverse and longitudinal beam velocity spreads. If the neglect of beam space charge turns out to be a significant error, there would be some recourse (e.g., larger number of beams or use of lead ions instead of Xenon) at the expense of some possible increase in cost.

More recently, Debbie Callahan has been able to reduce the required fast ignition energy to

$E_{ig2} := 228 \cdot 10^3$ (J), by reducing the ion range to 1.3 g/cm^2 : $T_{f2} := 16 \cdot 10^9$ (eV) for Xenon.

Despite the lower total energy, this case gives higher peak currents per beam

$I_f\left(E_{ig2}, T_{f2}, A, 1, N_b\right) = 5.7 \cdot 10^3$ (A), for q=1, and

$I_f\left(E_{ig2}, T_{f2}, A, 26, N_b\right) = 1.482 \cdot 10^5$ (A) for q=26, requiring better neutralization:

$\%F_{sc}\left(\theta_f, a_f, r_s, T_{f2}, 1, A, I_f\left(E_{ig2}, T_{f2}, A, 1, N_b\right)\right) = 55$ (%) for q=1, and

$\%F_{sc}\left(\theta_f, a_f, r_s, T_{f2}, 26, A, I_f\left(E_{ig2}, T_{f2}, A, 26, N_b\right)\right) = 99.93$ (%), for q = 26.

We also find (below) that $\delta p/p$ spread for a given ΔT_{par} is less by a $\beta^2\gamma$ factor which favors higher energies for focusing to the required spot size. Thus, despite the lower ignition energy possible with the lower range case, this memo will try to evaluate focusing at the higher 4 g/cm^2 range.

Scaling formulas for the target spot size in terms of ε_n and $\delta p/p$

With T ~ T_{par} the total kinetic ion energy (in eV), and A the atomic number, the transverse beam temperature ΔT_{perp} determines the normalized beam emittance:

$$\varepsilon_n\left(T, \Delta T_{perp}, A, a_b\right) := 2 \cdot \gamma(T, A) \cdot a_b \cdot \sqrt{\frac{e \cdot \Delta T_{perp}}{A \cdot M_p \cdot c^2} \cdot 10^6} \quad (\pi \text{ mm-mr}), \qquad \text{Eq. 4}$$

where a_b is the beam radius (m) at the some point where ΔT_{perp} (in eV) is measured.

The parallel temperature ΔT_{par} out of the accelerator, together with the beam drift compression ratio C_{dr} after acceleration, determines the normalized momentum spread at the final focus lens:

$$\delta p_p\left(T,\Delta T_{par},A,C_{dr}\right) := \left(\frac{e\cdot\Delta T_{par}}{A\cdot M_p\cdot c^2}\right)\cdot\frac{C_{dr}}{\beta(T,A)^2\cdot\gamma(T,A)} \qquad \begin{matrix}(= \text{delta p / p} \\ \text{at final focus).}\end{matrix} \qquad \text{Eq.5}$$

In terms of these transverse and parallel measures of beam quality at the final focus with magnets at distance L_f from the target, the beam spot size at the target, (again, neglecting space charge effects), is given by

$$r_s\left(T,\Delta T_{perp},\Delta T_{par},A,a_b,L_f,\theta_f,C_{dr}\right) := \left[\left(\frac{\varepsilon_n\left(T,\Delta T_{perp},A,a_b\right)\cdot 10^{-6}}{\beta(T,A)\cdot\gamma(T,A)\cdot\theta_f}\right)^2 \ \ldots \right.$$
$$\left. + \left(6\cdot L_f\cdot\theta_f\cdot\delta p_p\left(T,\Delta T_{par},A,C_{dr}\right)\right)^2\right]^{0.5} \quad (m), \quad \text{Eq.6}$$

In Eq. 5 and 6, any contribution to $\delta p/p$ at final focus due to residual coherent velocity tilt is omitted, as aberration due to a small velocity tilt through the lens is assumed to be corrected by a rising e-beam pulse counter-injected for this purpose. Such a fast correction optic will be described later on.

This spot size is minimized at a particular focusing angle $\theta_f = a_f / L_f$ given by

$$\theta_f\left(T,\Delta T_{perp},\Delta T_{par},A,a_b,L_f,C_{dr}\right) := \sqrt{\frac{\varepsilon_n\left(T,\Delta T_{perp},A,a_b\right)\cdot 10^{-6}}{\beta(T,A)\cdot\gamma(T,A)\cdot 6\cdot L_f\cdot\delta p_p\left(T,\Delta T_{par},A,C_{dr}\right)}} \qquad \text{Eq. 7}$$

and with this focusing angle, the minimum spot size becomes

$$r_{sm}\left(T,\Delta T_{perp},\Delta T_{par},A,a_b,L_f,C_{dr}\right) := \sqrt{\frac{\varepsilon_n\left(T,\Delta T_{perp},A,a_b\right)\cdot L_f\cdot\delta p_p\left(T,\Delta T_{par},A,C_{dr}\right)}{0.0833\cdot\beta(T,A)\cdot\gamma(T,A)\cdot 10^6}}$$

(m) Eq.8

Transverse emittance:

Assuming a well-matched beam transported in a quadrupole FODO lattice, the transverse temperature ΔT_{perp} derives from the source ion temperature T_s, from induced nonlinearities in the beam space charge fields arising from the beam encountering both magnet misalignments within the accelerator and electrons in-flows outside the accelerator during beam neutralization, and from non-linear focusing elements in which beams with radii a_b approaching the lens apertures sample nonlinear fringe fields, such as with electrostatic lens (Pierce electrodes and ESQ's) and magnetic quadrupoles. Generally, one can spend money to reduce the beam aperture fill factors and magnet misalignments for the lower beam energies needed for this application, and one can increase the number of beams (to reduce the current per beam) to reduce those sources of beam emittance that grow with the beam line-charge density, but after that is done a practical ion source temperature and source radius is often viewed as a fundamental minimum contributor to beam transverse emittance. For this excercise, we will assume that the transverse emittance due to the source is characterized by:

$\Delta T_{perp} := 20$ (eV), (always higher than the actual ion source temperature due to source non-uniformities), and by a beam radius at the source

$a_b := 10^{-2}$ (m), (nominal size for ~ an amp in high gradient gaps).

Later on, the source radius a_b will be adjusted to provide the required source current depending on ion mass and charge state. These assumptions give a normalized transverse emittance [weakly dependent on injector energy thru the γ factor in Eq. 4] :

$$\varepsilon_n\left(10^6, \Delta T_{perp}, 131, a_b\right) = 0.25 \qquad (\pi \text{ mm-mr}),$$

which is about equal to the best normalized emittances that have been achieved in sources that have been built at LLNL and LBNL. Many studies assume at least a doubling of the source emittance to provide an allowance for the other mechanisms for emittance growth described above that are not calculated. Here, we will simply use a higher effective source temperature of 4 x ΔT_{perp}, carrying an explicite factor of 4 as a reminder; so for this example,

$$\varepsilon_n\left(10^6, 4\cdot\Delta T_{perp}, 131, a_b\right) = 0.51 \qquad (\pi \text{ mm-mr}).$$

With laser-produced plasma ion sources, it is possible to allow pre-plasma expansion to cool the source ion temperature below 0.1 eV before extraction (See "Model for High-Charge-State Ion induction Accelerators" by Logan, Perry and Caporaso, UCRL-ID-126815, Feb. 25, 1997). Only a small solid-angle fraction of such expanding ions can be used for a low-aberration beam (Oscar Anderson's Heidelberg paper), on the other hand, this may be acceptable since far fewer ions are needed per pulse for this high ion-range target. This advanced source possibility will be held in reserve if needed later. It will also be important to perform more detailed calculations of the other possible emittance growth mechanisms that are assumed here to be limited to doubling of the initial source emittance.

Parallel momentum spread: The sources of beam longitudinal velocity spread are (1) variations of voltage on the injector, (2) transfer of perpendicular energy spread to parallel spread by instabilities where $\Delta T_{perp} >> \Delta T_{par}$ near the injector, (3) growth of longitudinal instabilities (space-charge waves) due to beam-induction gap coupling, and (4) random pulser variations (noise) on the induction module's accelerating voltages.

For (1), it is believed to be possible to spend money to make the injector voltage flat enough to be ignorable (requireing tight control on one pulser), (2) coupling instabilities saturate when ΔT_{par} reaches about 0.5 ΔT_{perp} near the injector, but that initial longitudinal velocity spread usually turns out to be less than due to (4), even after beam length compression by, say, 100 x. (recirulator example). (3) is thought to be controlled by proper design, such that the longitudinal mode does not grow fast enough to matter (Debbie Callahans work of several years ago). (4) Cumulative longitudinal beam heating by the beam crossing thousands of acceleration gaps, multiplied by the drift compression ratio of the beam length after acceleration, is thought to be the primary mechanism for δp spread at final focus. It is believed that reproducable parts of pulser voltage variations can be corrected for down to about the 0.1 % level by addition of "smart" trim cores driven by amplifier-mode FET switches (Lou Reginato, DARHT II concept), but then there is always left some stochastic part. The following simple model attempts to provide a scaling for the remaining (assumed stochastic) variations in pulser voltages, characterized by a dimensionless parameter δV_{Vp} which in effect is economically limited to be greater than some small value.

Assuming the final desired ion kinetic energy T_f is provided by a number N_g of equal voltage gaps along the accelerator with $V_{gap} = T_f / (q\ N_g)$, with q being the ion charge state, and assuming that the imparted energy variations $q\delta V_p$ per gap are uncorrelated, the parallel energy spread ΔT_{par} would grow as the square of the number of gaps crossed by the beam in the accelerator, multiplied by some "effective" beam length compression ratio C_{ar} within the accelerator, and multiplied by another drift compression ratio C_{dr} beyond the accelerator to the final focus lens. "Effective" is the adjective used for a characteristic C_{ar} because longitudinal heating and beam compression occur together distributed along the accelerator. We arbitrarily put the C_{dr} multiplier in Eq. 5 for δp_p at the final focus, so that ΔT_{par} below is representative of the value coming out of the accelerator.

$$\Delta T_{par}(T_f, N_g, \delta V_{Vp}, C_{ar}) := T_f \cdot N_g^{-0.5} \cdot \delta V_{Vp} \cdot C_{ar} \quad \text{(eV), end of accelerator)} \quad \text{Eq. 9}$$

The required number of gaps is $N_g(T_f, q) := T_f \cdot (2 \cdot 10^5 \cdot q)^{-1}$ (@ 200 kV/gap) Eq. 10

Example of this model for a "conventional" heavy-ion linac: 4 GeV Pb^{+1}, 1% pulser regulation, $C_{ar} = 4$, and $C_{dr} = 20$, with ΔT_{perp} and a_b increased to "fill-up" transverse emittance budget:

$N_g(4 \cdot 10^9, 1) = 2 \cdot 10^4$ gaps, $\Delta T_{par}(4 \cdot 10^9, 2 \cdot 10^4, 10^{-2}, 4) = 1.1 \cdot 10^6$ (eV)

$\delta p_p(4 \cdot 10^9, 1.1 \cdot 10^6, 207, 20) = 2.8 \cdot 10^{-3}$ ($\delta p/p$)

$r_{sm}(4 \cdot 10^9, 1000, 1.1 \cdot 10^6, 207, 0.025, 5, 20) = 1.7 \cdot 10^{-3}$ (m), spot on target @ 5 m

$\theta_f(4 \cdot 10^9, 1000, 1.1 \cdot 10^6, 207, 0.025, 5, 20) = 0.015$ (radians), for best focus

--> all familiar answers! [the model reproduces conventional HIF parameters].

For fast ignition, we take a goal of 10 better regulation than required for "conventional" HIF designs, and this implies some active or passive (feed back or feed forward) corrections for voltage ripple

$$\delta V_{Vp} := 10^{-3}$$

As the pulses will be much shorter in fast ignition linacs, we take the maximum acceleration gradient to be twice the 2 MV/m value assumed in the Heidelberg baseline design (Meier, Bangerter, Faltens). At a maximum voltage gradient along the accelerator

$$V_{gm} := 4 \cdot 10^6 \qquad \text{(V/m)},$$

there would be 20 gaps per meter, each gap ~ 1 cm at 2x10^5 V/cm, leaving an average of 4 cm spaces between the gaps. As we will see, quadrupole focusing is so effective at the higher ion velocities, scaling as $(\beta\gamma)^2$, that focusing quadrupoles can become very sparse (one every many gaps) at the high energy end of the linac. To minimize transport mismatches, the acceleration gradient is assumed to ramp up to the above maximum value slowly enough that the beam energy gain in a beam length is less than a factor of two near the injector end:

$$V_g(T, q, L_{bo}) := \frac{T \cdot \left[q \cdot (L_{bo})\right]^{-1}}{1 + T \cdot \left[q \cdot (L_{bo})\right]^{-1} \cdot V_{gm}^{-1}} \qquad \text{(V/m)}, \quad \text{Eq. 11}$$

where $L_{bo} = \beta_o c \tau_o$ is the initial beam length out of the injector. An example is plotted in Fig.1 below.

For $V_s := 2 \cdot 10^6$ volt injection of $q := 26$ Xenon ions for $\tau_o := 900 \cdot 10^{-9}$ (s) duration, initial beam length is $L_{bo} := \beta(q \cdot V_s, A) \cdot c \cdot \tau_o$ $L_{bo} = 7.8$ (m).

For a final $T_f = 4 \cdot 10^{10}$ (eV) and $i := 1 .. 20000$ points plotted, $T_i := q \cdot V_s + i \cdot \frac{T_f - q \cdot V_s}{20000}$

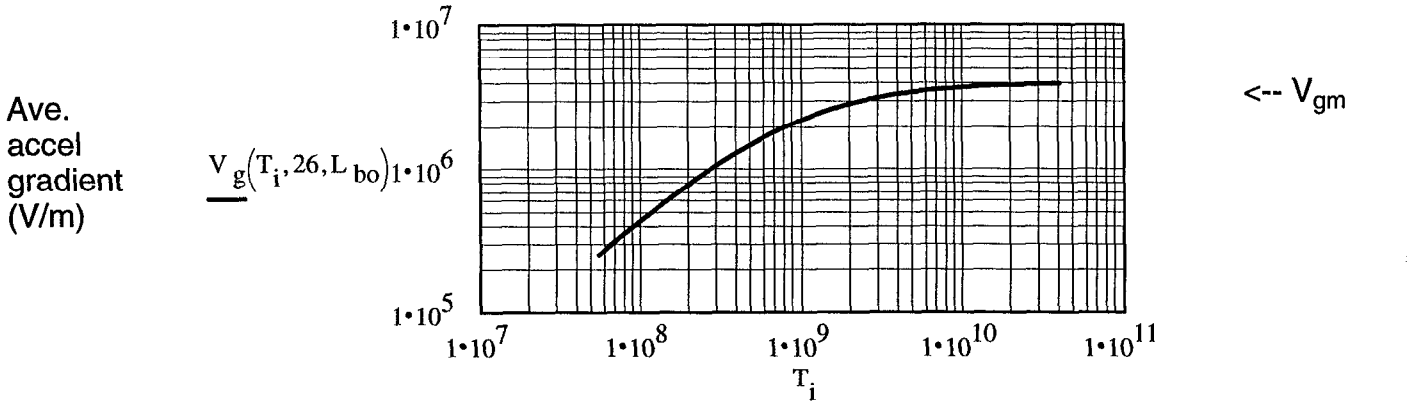

Fig. 1: Average acceleration gradient (V/m) versus ion kinetic energy T in eV.

The beam lengths at the high gradient end will be also be more than 10 x shorter here than in conventional HIF designs (e.g, 0.4 m instead of 9 meters), so the maximum induction voltage drops over a beam length will still be less at the higher maximum gradient above than in conventional HIF designs at half the gradient. To provide more axial insulation space along the induction cores at such a high gradient, we might arrange the cores for each gap to be supplied in external 20 cm long, 200 kV voltage adder modules with a moderate 1 MV/m average gradient along each module. The power from each voltage adder module could be fed via equal length coaxial cables to each gap consisting of a radial transmission line with hole patterns for multible beams to pass through, as illustrated schematically in Fig. 2 below. The radial build of such cores would be very small at the short pulses envisioned at the high energy end, e.g, at ~10 ns: Δr_{core} ~ 10^6 (V/m) x 10^{-8} sec / 0.4 T ~ 2.5x10^{-2} m assuming ΔB = 0.5 T flux swing for ferrite, and 0.8 packing fraction. Thus, the voltage-adder modules can be small enough in diameter to be placed in a spiral array staggered in z and in azimuth around a linac to achieve 4 MV/m ave. gradient (possibly higher) along the linac.

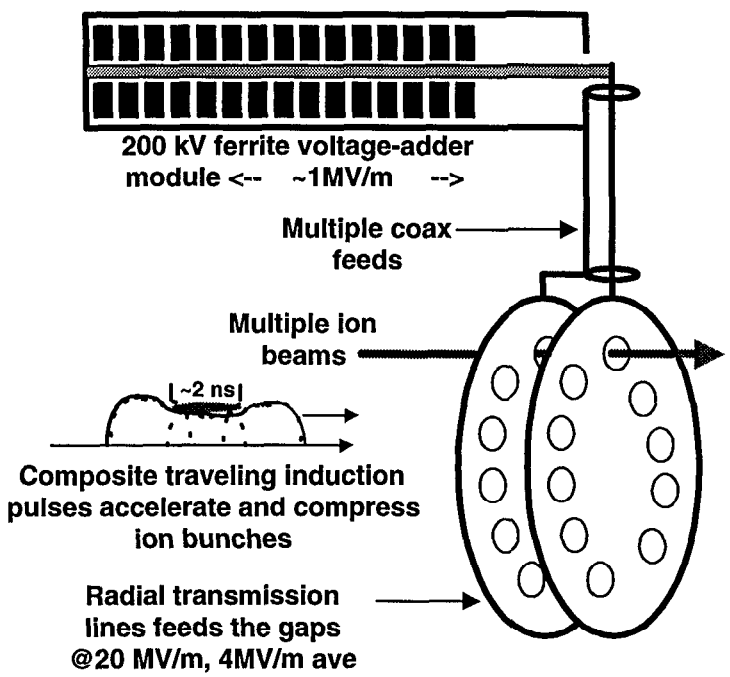

Fig.2 Schematic of a high-gradient induction linac using voltage-adder modules staggered in z and azimuth around the linac. To minimize switching (FET) costs, the voltage adder cores may be driven by one or two stages of magnetic pulse compression (like ETA-II). Individual ferrite cores in the voltage adder module may vary in amplitude and phase to achieve control of the the module output waveform, e.g., to create a central dip in the waveform to confine, accelerate, and axially compress short ion bunches in a tailored traveling induction pulse. The induction pulse can be several times longer than the ion bunch at the high energy end.

Longitudinal beam confinement constraint on beam compression

For a given longitudinal heating ΔT_{par}, a lower $\delta p/p$ would result from first compressing a beam to a short length and then heating (adding ΔT_{par}), compared to heating and then compressing the length. Thus, for the smallest parallel spread at final focus, we want to accomplish as much of the overall beam length compression within the accelerator as possible, minimizing drift compression after acceleration. To the degree allowed by constraints on both ends of the accelerator, one would compress the beam length as it accelerates beyond the injector according to $L_b(z) \sim L_{bo}\, \beta_o / \beta(z)$, which leads to a beam current increasing along the accelerator as $I_s\, (\beta/\beta_o)^2$.

In regions of the accelerator where it is possible to compress the beam with the above scaling, the beam current will rise as fast as the maximum transportable current with a given quadrupole occupancy factor, which current limit also scales as β^2. However, this scaling causes the longitudinal beam space charge electric field $E_z \sim 4\Delta\phi / L_b \sim 4\, I_b / (4\pi\varepsilon_o\, \beta c\, L_b)$ to also grow as β^2, so that in some cases E_z could exceed the maximum longitudinal induction voltage gradient, at which point the ion bunches cannot be longitudinally confined in practical pulse shapes as depicted in Fig. 2 above. (The factor of 4 in E_z accounts for an assumed parabolic axial beam line charge density). We therefore impose a constraint on the beam current such that E_z never exceeds some fraction, say, one third, of the local average induction gradient given by Eq. 11. This constraint occurs first, if at all, at the highest energy end of the accelerator. Given a desired current and charge per beam derived from Eq. 1, a condition on minimum beam length at the ouptut end of the linac can be determined from a constraint that $E_z < 0.3\, V_{gm}$ there :

$$L_{ba}(I_s, \tau_o) := \sqrt{\frac{I_s \cdot \tau_o}{\pi \cdot \varepsilon_o \cdot 0.3 \cdot V_{gm}}} \quad \text{(m).} \qquad \text{Eq. 12}$$

where I_s is the injector (source) current, and τ_o is the injector pulse duration. The beam length will be longer than L_{ba} at the injector, which can be compressed down to the limit of L_{ba} given by Eq. 12.

Drift compression after acceleration.

Most conventional HIF designs provide a small coherent velocity tilt $\delta v_z/v_z \sim 1$ to 4 % (beam tail going faster than the head of the beam) imposed on the beam exiting the accelerator, to drift compress the beam length between the linac output and the final focus lens by a factor of

$$C_{dr} := 10$$

after acceleration, in a drift distance $L_d \sim L_{ba} / (\delta v_z/v_z)$. The tilt is usually chosen so that the longitudinal beam space charge field removes the velocity tilt by the time the beam gets to the final focus magnets, to avoid chromatic aberrations with static focusing magnets. However, because of the very high kinetic energy of ions required for fast ignition, coupled with the limit on longitudinal beam fields $E_z < 4\text{x}10^6$ V/m implied by Eq. 11 at the beginning of drift compression, the maximum allowed velocity tilt is very small. The reduction in kinetic energy for a tail ion by longitudinal space charge fields over a drift length compression ratio C_{dr} =10 is given by $\delta T_{tail} = qE_zL_{ba}(C_d\text{-}1) \sim 4\text{x}10^6 \text{ x } 0.3 \text{ x } 9 \sim 11$ MeV for q=1 ions, or 280 MeV for q =26 ions, limiting initial velocity tilts $\delta v_z/v_z$ to $1.4\text{x}10^{-4}$ for q=1, or $3.6\text{x}10^{-3}$ for q=26. The implied drift lengths for an initial beam length of 0.4 m are 2900 m and 111 m, respectively. While the drift length at q =26 would be acceptable, the implied beam potential at peak compression $\Delta\phi = C_{dr} \text{ x } 4\text{x}10^6$ V/m x0.4m = 16 MV is much too high -will likely trigger breakdown on the final focus magnet channel walls. Thus, un-neutralized beam drift compression to get a space-charge bounce for velocity tilt removal leads either to very long drift distances at low q, or to breakdown at high q.

One concludes that beam space-charge neutralization, as was discussed above, has to begin upstream of the target chamber, somewhere after acceleration, but well before peak drift compression. As a further consequence of neutralized drift compression, the coherent velocity tilt will persist through the final focus magnet, and so chromatic aberration has to compensated with some kind of fast time-varying optic correction. Fortunately, the percentage focusing field change can be as small as the required velocity tilt for drift compression of short beams, say, 0.5%. Still, the required rates of change are too fast for conventional focusing magnets.

A solution is suggested by the observation that small cold electron flow energy provides substantial beam space-charge and current neutralization in Callahan's PIC calculations of chamber beam neutralization using cold electron sources at the ion beam entrance into the target chamber. Thus, if we could control the spatial and temporal profiles of a rising e-beam pulse of similar currents injected into the ion beam channel after the final focus magnet, we could in principle correct for chromatic aberration due to small coherent velocity tilts. Fig. 3 below sketches a conceptual e-beam correction optic scheme for this purpose.

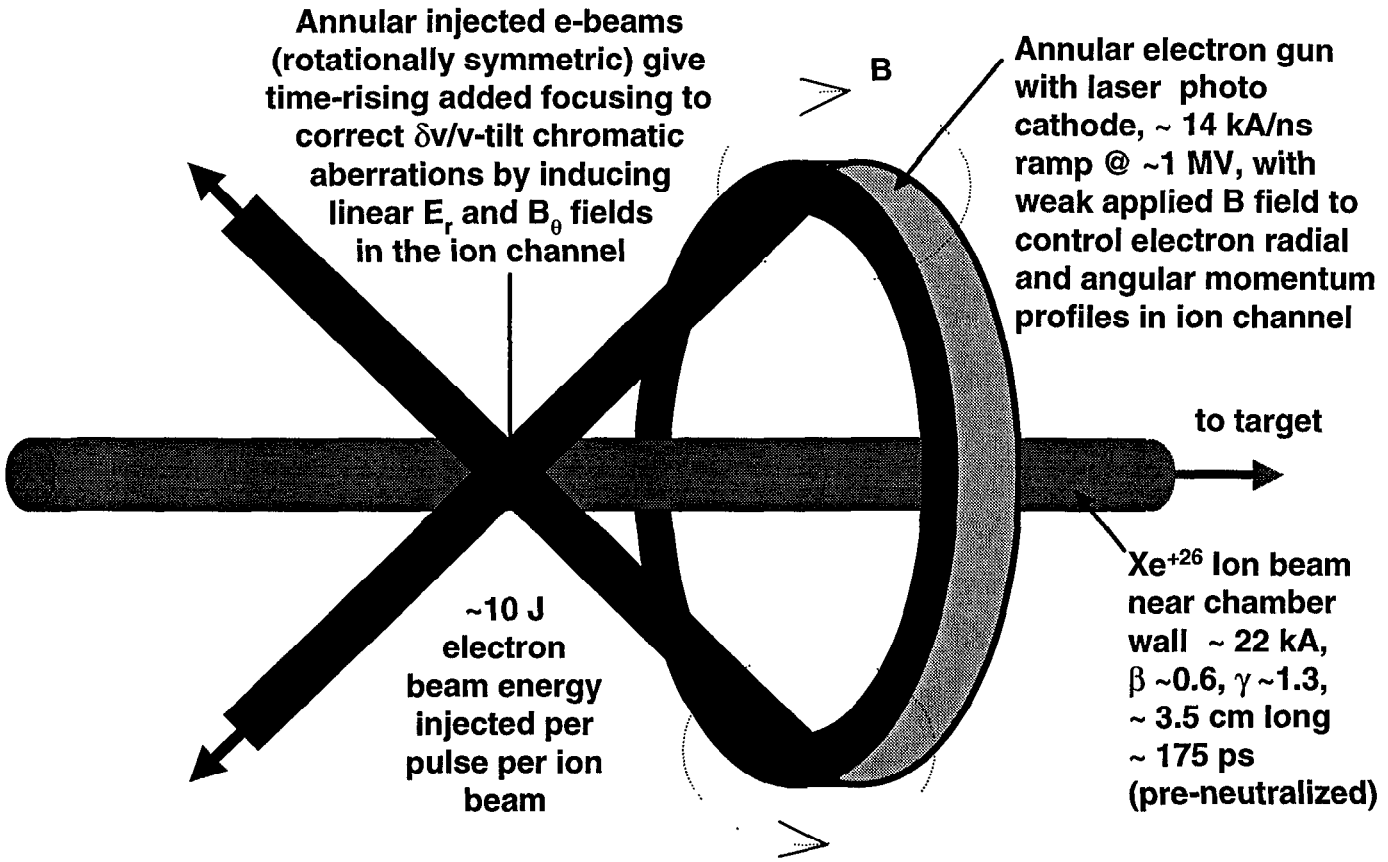

Fig. 3 A conceptual fast focusing optic to correct chromatic aberrations due to coherent residual δv/v tilt (~0.5 %) through a prior static focusing lens. Fast rising electron beams (14kA/ns) provide tailored E_r and B_θ fields increasing over 175 ps beam passage. Tailoring the applied B in the diode controls radial profiles through the angular momentum imparted to the electrons.

For a nominal 10 mr static focusing half-angle and a 0.5% velocity tilt, the e-beam current increase over a 175 ps beam pulse required to add a 5×10^{-5} radian focusing correction to the beam tail is estimated to be

$$I_e(T_f, A, q) := 5 \cdot 10^{-5} \cdot \frac{M_p \cdot A \cdot \gamma(T_f, A) \cdot \beta(T_f, A) \cdot c}{q \cdot e \cdot \mu_o} \cdot \pi \cdot \sin\left(\frac{\pi}{4}\right)^{-1} \qquad \text{Eq.13}$$

For our Xe^{+26} case $I_e(T_f, A, 26) = 2.4 \cdot 10^3$ (Amps), for $T_f = 4 \cdot 10^{10}$ (eV)

The required rate of rise of the e-beam current is $\frac{I_e(T_f, A, 26)}{175 \cdot 10^{-12}} = 1.4 \cdot 10^{13}$ (Amps/sec).

A gun voltage of about 1 MV is required to provide this rate of rise of current (Ldl/dt drop), but only for very short pulses, hence only a few joules per pulse are required.

The actual e-beam currents required are probably a factor of two less (~7 kA/ns), because the electrostatic forces due to elecron injection, which were neglected, are comparable to the induced magnetic forces. Detailed simulations can later determine the desired electron beam spatial and temporal profiles required for chromatic aberration correction. Incidentally, to the same degree, such an electron beam optic can also be used to correct geometric aberrations in cylindrically symmetric upstream static lens such as solenoids or plasma (z-pinch) lens. It should also be noted that a 0.5% velocity tilt corresponds to a tail $\delta v \sim 10^8$ cm/s faster than the beam head, so that the beam pulse traveling 5 m from the final focus lens to the target shrinks from 3.5 cm and 175 ps at the final focus lens, to 1 cm and 50 ps at the target. Debbie Callahan has shown that the ignition energy drops from 650 kJ at 156 ps to 300 kJ at 50 ps. Thus we make a virtue of a necessity (fast correction optic for focusing with a velocity tilt). We will keep τ_f = 175 ps to be the pulse length at the final focus lens, with 50 ps at the target.

Injector and other accelerator parameters

Using $I_s \tau_o = \pi \varepsilon_o 0.3 V_{gm} L_{ba}^2$ obtained from Eq.12, setting $L_{ba} = 3.5\, \tau_f C_{dr} \beta_f c$, and then setting $I_s \tau_o = q E_{ig} / (N_b T_f)$, one gets an expression for the required number of beams:

$$N_b(T_f, q, A) := \frac{q \cdot E_{ig}}{3.5^2 \cdot \pi \cdot \varepsilon_o \cdot 0.3 \cdot V_{gm} \cdot \tau_f^2 \cdot C_{dr}^2 \cdot \beta(T_f, A)^2 \cdot c^2 \cdot T_f} \qquad \text{Eq. 14}$$

For our Xe+26 example $N_b(T_f, q, A) = 49$

Since we want to minimize overall beam length compression ratios (to limit build-up of $\delta p/p$ spread at final focus), we prefer short pulses at the injector, which, for a given number of beams given by Eq. 14 and charge per beam, are reduced by larger source currents, which increases in turn with higher diode voltages (for simplicity, no ESQ section is assumed here). Thus, we take a nominal source (injection) voltage of

$V_s := 2 \cdot 10^6$ (Volts)

Using a fixed diode gap aspect ratio $A_d = d/a_s$ (high for good beam quality) $A_d := 7$

the source current is

$$I_s(q, A) := 5.46 \cdot 10^{-8} \cdot \frac{\pi}{A_d^2} \cdot \sqrt{\frac{q}{A} \cdot V_s^3} \quad \text{(Amps)}, \qquad \text{Eq. 15}$$

$I_s(q, A) = 4.4$ (A)

The injector pulse duration required to deliver the charge per beam is then

$$\tau_o(T_f,q,A) := \frac{q \cdot E_{ig}}{N_b(T_f,q,A) \cdot I_s(q,A) \cdot T_f} \quad \text{(sec)} \qquad \text{Eq 16}$$

$$\tau_o(T_f,q,A) = 9 \cdot 10^{-7} \quad \text{(s)}$$

and the corresponding beam length out of the injector is:

$$L_{bo}(T_f,q,A) := \tau_o(T_f,q,A) \cdot \beta(q \cdot V_s,A) \cdot c \quad \text{(m)} \qquad \text{Eq. 17}$$

$$L_{bo}(T_f,q,A) = 7.8$$

With shorter injector pulses, the diode gap gradient can be higher as 10^7 (V/m)(20μs/ τ_o)$^{0.2}$, giving a source radius

$$a_s(T_f,q,A) := V_s \cdot \left[10^7 \cdot \left(\frac{2 \cdot 10^{-5}}{\tau_o(T_f,q,A)} \right)^{0.2} \cdot A_d \right]^{-1} \quad \text{(m)} \qquad \text{Eq. 18}$$

$$a_s(T_f,q,A) = 0.015 \quad \text{(m)}$$

The beam length at the accelerator output end is

$$L_{ba}(T_f,q,A) := \sqrt{\frac{I_s(q,A) \cdot \tau_o(T_f,q,A)}{\pi \cdot \varepsilon_o \cdot 0.3 \cdot V_{gm}}} \quad \text{(m)} \qquad \text{Eq. 19}$$

$$L_{ba}(T_f,q,A) = 0.344 \quad \text{(m)}$$

For the effective beam length compression ratio, we take the square root of the beam length ratio (injector beam length over exit beam length), since longitudinal heating and compression is distributed along the accelerator:

$$C_{ar}(T_f,q,A) := \sqrt{\frac{L_{bo}(T_f,q,A)}{L_{ba}(T_f,q,A)}} \qquad C_{ar}(T_f,q,A) = 4.8 \qquad \text{Eq. 20}$$

The beam pulse duration at the accelerator output end is

$$\tau_a(T_f,q,A) := \frac{L_{ba}(T_f,q,A)}{\beta(T_f,A) \cdot c} \quad \text{(s)} \qquad \text{Eq. 21}$$

$$\tau_a(T_f,q,A) = 1.75 \cdot 10^{-9} \quad \text{(s)}$$

The beam current at the accelerator output end

$$I_a(T_f,q,A) := I_s(q,A) \cdot \frac{L_{bo}(T_f,q,A)}{L_{ba}(T_f,q,A)} \cdot \frac{\beta(T_f,A)}{\beta(q \cdot V_s,A)} \quad \text{(A)} \qquad \text{Eq. 22}$$

$$I_a(T_f,q,A) = 2.3 \cdot 10^3 \quad \text{(A)}$$

The total accelerator length, with V_g (Eq. 11) ramped to keep $qV_g(z)L_b(z)<T(z)$ at any point z, is

$$L_a(T_f,q,A) := \int_{q\cdot V_s}^{T_f} \frac{1 + T\cdot\left[q\cdot\left(\tau_o(T_f,q,A)\cdot\beta(q\cdot V_s,A)\cdot c\right)\right]^{-1}\cdot V_{gm}^{-1}}{T\cdot\left[q\cdot\left(\tau_o(T_f,q,A)\cdot\beta(q\cdot V_s,A)\cdot c\right)\right]^{-1}\cdot q} dT \quad (m) \qquad \text{Eq.23}$$

III. Comparison of candidate ion masses and charge states

We next will evaluate several ion masses and charge states, for the common models, assumptions, and target requirements described above. Comparisons of these cases will be summarized in Table 1 several pages further on. Each ion species is evaluated for both a low charge state (q=1) and a higher charge state at shell jumps that increase with atomic mass. The achievable spot sizes due to the same model for emittance and longitudinal spreads is evaluated for each case. The achievable target spot size is evaluated subject to constraints that all cases have the same ion range, total beam energy delivered, final pulse duration at the final focus position and at the target, fixed source/injector ion temperature, diode aspect ratio and voltage, ratio of longitudinal electric field to voltage gradient, pulser fluctuation level, and drift compression ratio C_{dr}. Shown in Fig. 4 below are the kinetic energies for each species required for a "conventional" HIF target using distributed radiators with range R~0.4 g/cm^2, and for these fast ignitor cases with R = 0.4 g/cm^2.

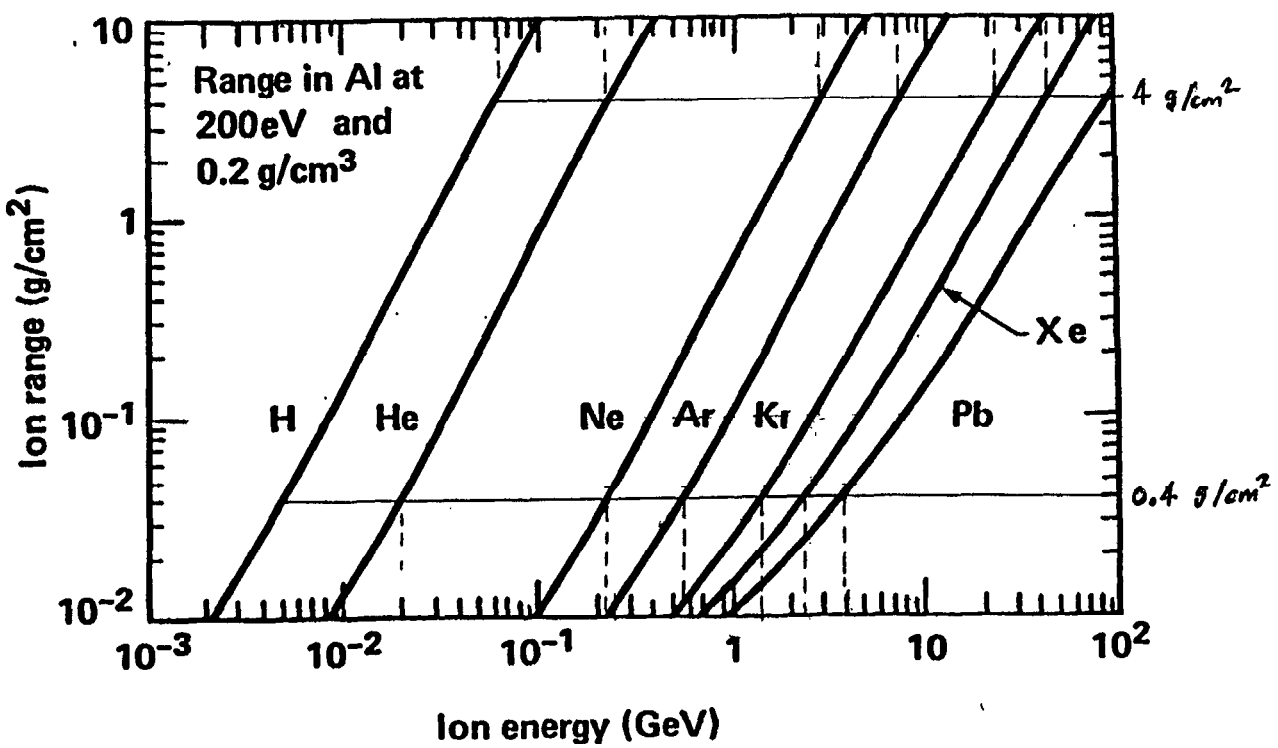

Figure 4. Ion range versus ion kinetic energy for various ion masses used in the comparative ion survey. This figure may underpredict the required ion kinetic energy for a given range by ~10%. However, the relative values are good enough for the comparative analysis here.

Case 1.1 :Helium-low q

Atomic mass $A_1 := 4$ Final ion energy for R=4g/cm^2 $Tf_1 := 2.2\cdot10^8$ (eV)

Final ion beta $\beta(Tf_1, A_1) = 0.33$ Final ion gamma $\gamma(Tf_1, A_1) = 1.06$

Charge state $q_{1,1} := 1$ Charge to mass ratio $q_{1,1}\cdot(A_1)^{-1} = 0.25$

Accelerator length

$La_{1,1} := L_a(Tf_1, q_{1,1}, A_1)$ $La_{1,1} = 64$ (m)

Source current per beam

$Is_{1,1} := I_s(q_{1,1}, A_1)$ $Is_{1,1} = 5$ (A)

Injection pulse length

$\tau o_{1,1} := \tau_o(Tf_1, q_{1,1}, A_1)$ $\tau o_{1,1}\cdot10^9 = 200$ (ns)

Number of beams

$Nb_{1,1} := N_b(Tf_1, q_{1,1}, A_1)$ $Nb_{1,1} = 1.4\cdot10^3$

Injected beam length

$Lbo_{1,1} := L_{bo}(Tf_1, q_{1,1}, A_1)$ $Lbo_{1,1} = 2$ (m)

Injector source radius

$as_{1,1} := a_s(Tf_1, q_{1,1}, A_1)$ $as_{1,1} = 0.011$ (m)

Beam length at end of accelerator

$Lba_{1,1} := L_{ba}(Tf_1, q_{1,1}, A_1)$ $Lba_{1,1} = 0.172$ (m)

Current/beam at end of the accelerator

$Ia_{1,1} := I_a(Tf_1, q_{1,1}, A_1)$ $Ia_{1,1}\cdot10^{-3} = 0.57$ (kA)

"Effective" beam compression ratio in accelerator

$Car_{1,1} := C_{ar}(Tf_1, q_{1,1}, A_1)$ $Car_{1,1} = 3.4$

Number of voltage gaps @ 200 kV/gap

$Ng_{1,1} := N_g(Tf_1, q_{1,1})$ $Ng_{1,1} = 1.1\cdot10^3$ gaps

Parallel beam temperature at end of accelerator

$\Delta Tpar_{1,1} := \Delta T_{par}(Tf_1, Ng_{1,1}, \delta V_{Vp}, Car_{1,1})$ $\Delta Tpar_{1,1} = 2.2\cdot10^4$ (eV)

Transverse beam emittance 2x source emittance

$\varepsilon n_{1,1} := \varepsilon_n(Tf_1, 4\cdot\Delta T_{perp}, A_1, as_{1,1})$ $\varepsilon n_{1,1} = 3.51$ π mm-mr

Normalized longitudinal momentum spread at final focus

$\delta pp_{1,1} := \delta p_p(Tf_1, \Delta Tpar_{1,1}, A_1, C_{dr})$ $\delta pp_{1,1} = 5.2\cdot10^{-4}$ (delta p/p)

Best final focusing angle

$\theta f_{1,1} := \theta_f(Tf_1, 4\cdot\Delta T_{perp}, \Delta Tpar_{1,1}, A_1, as_{1,1}, L_f, C_{dr})$ $\theta f_{1,1}\cdot10^3 = 25$ (mrad)

Minimum spot radius on target

$rsm_{1,1} := r_{sm}(Tf_1, 4\cdot\Delta T_{perp}, \Delta Tpar_{1,1}, A_1, as_{1,1}, L_f, C_{dr})$ $rsm_{1,1}\cdot10^6 = 563$ (μm)

Case 1.2 :Helium-high q

Atomic mass $A_1 := 4$ Final ion energy for R=4g/cm^2 $Tf_1 := 2.2\cdot10^8$ (eV)

Final ion beta $\beta(Tf_1, A_1) = 0.33$ Final ion gamma $\gamma(Tf_1, A_1) = 1.06$

Charge state $q_{1,2} := 2$ Charge to mass ratio $q_{1,2}\cdot(A_1)^{-1} = 0.5$

Accelerator length

$La_{1,2} := L_a(Tf_1, q_{1,2}, A_1)$ $La_{1,2} = 35$ (m)

Source current per beam

$Is_{1,2} := I_s(q_{1,2}, A_1)$ $Is_{1,2} = 7$ (A)

Injection pulse length

$\tau o_{1,2} := \tau_o(Tf_1, q_{1,2}, A_1)$ $\tau o_{1,2}\cdot10^9 = 141$ (ns)

Number of beams

$Nb_{1,2} := N_b(Tf_1, q_{1,2}, A_1)$ $Nb_{1,2} = 2.8\cdot10^3$

Injected beam length

$Lbo_{1,2} := L_{bo}(Tf_1, q_{1,2}, A_1)$ $Lbo_{1,2} = 1.95$ (m)

Injector source radius

$as_{1,2} := a_s(Tf_1, q_{1,2}, A_1)$ $as_{1,2} = 0.011$ (m)

Beam length at end of accelerator

$Lba_{1,2} := L_{ba}(Tf_1, q_{1,2}, A_1)$ $Lba_{1,2} = 0.172$ (m)

Current/beam at end of the accelerator

$Ia_{1,2} := I_a(Tf_1, q_{1,2}, A_1)$ $Ia_{1,2}\cdot10^{-3} = 0.57$ (kA)

"Effective" beam compression ratio in accelerator

$Car_{1,2} := C_{ar}(Tf_1, q_{1,2}, A_1)$ $Car_{1,2} = 3.4$

Number of voltage gaps @ 200 kV/gap

$Ng_{1,2} := N_g(Tf_1, q_{1,2})$ $Ng_{1,2} = 550$ gaps

Parallel beam temperature at end of accelerator

$\Delta Tpar_{1,2} := \Delta T_{par}(Tf_1, Ng_{1,2}, \delta V_{Vp}, Car_{1,2})$ $\Delta Tpar_{1,2} = 3.2\cdot10^4$ (eV)

Transverse beam emittance 2x source emittance

$\varepsilon n_{1,2} := \varepsilon_n(Tf_1, 4\cdot\Delta T_{perp}, A_1, as_{1,2})$ $\varepsilon n_{1,2} = 3.28$ π mm-mr

Normalized longitudinal momentum spread at final focus

$\delta pp_{1,2} := \delta p_p(Tf_1, \Delta Tpar_{1,2}, A_1, C_{dr})$ $\delta pp_{1,2} = 7.4\cdot10^{-4}$ (delta p/p)

Best final focusing angle

$\theta f_{1,2} := \theta_f(Tf_1, 4\cdot\Delta T_{perp}, \Delta Tpar_{1,2}, A_1, as_{1,2}, L_f, C_{dr})$ $\theta f_{1,2}\cdot10^3 = 21$ (mrad)

Minimum spot radius on target

$rsm_{1,2} := r_{sm}(Tf_1, 4\cdot\Delta T_{perp}, \Delta Tpar_{1,2}, A_1, as_{1,2}, L_f, C_{dr})$ $rsm_{1,2}\cdot10^6 = 647$ (μm)

Case 2.1: Neon-low q

Atomic mass $A_2 := 20.2$ Final ion energy for R=4g/cm^2 $Tf_2 := 2.7 \cdot 10^9$ (eV)

Final ion beta $\beta(Tf_2, A_2) = 0.48$ Final ion gamma $\gamma(Tf_2, A_2) = 1.14$

Charge state $q_{2,1} := 1$ Charge to mass ratio $q_{2,1} \cdot (A_2)^{-1} = 0.05$

Accelerator length

$La_{2,1} := L_a(Tf_2, q_{2,1}, A_2)$ $La_{2,1} = 705$ (m)

Source current per beam

$Is_{2,1} := I_s(q_{2,1}, A_2)$ $Is_{2,1} = 2.2$ (A)

Injection pulse length

$\tau o_{2,1} := \tau_o(Tf_2, q_{2,1}, A_2)$ $\tau o_{2,1} \cdot 10^9 = 975$ (ns)

Number of beams

$Nb_{2,1} := N_b(Tf_2, q_{2,1}, A_2)$ $Nb_{2,1} = 52$

Injected beam length

$Lbo_{2,1} := L_{bo}(Tf_2, q_{2,1}, A_2)$ $Lbo_{2,1} = 4.2$ (m)

Injector source radius

$as_{2,1} := a_s(Tf_2, q_{2,1}, A_2)$ $as_{2,1} = 0.016$ (m)

Beam length at end of accelerator

$Lba_{2,1} := L_{ba}(Tf_2, q_{2,1}, A_2)$ $Lba_{2,1} = 0.254$ (m)

Current/beam at end of the accelerator

$Ia_{2,1} := I_a(Tf_2, q_{2,1}, A_2)$ $Ia_{2,1} \cdot 10^{-3} = 1.23$ (kA)

"Effective" beam compression ratio in accelerator

$Car_{2,1} := C_{ar}(Tf_2, q_{2,1}, A_2)$ $Car_{2,1} = 4.1$

Number of voltage gaps @ 200 kV/gap

$Ng_{2,1} := N_g(Tf_2, q_{2,1})$ $Ng_{2,1} = 1.35 \cdot 10^4$ gaps

Parallel beam temperature at end of accelerator

$\Delta Tpar_{2,1} := \Delta T_{par}(Tf_2, Ng_{2,1}, \delta V_{Vp}, Car_{2,1})$ $\Delta Tpar_{2,1} = 9.5 \cdot 10^4$ (eV)

Transverse beam emittance 2x source emittance

$\varepsilon n_{2,1} := \varepsilon_n(Tf_2, 4 \cdot \Delta T_{perp}, A_2, as_{2,1})$ $\varepsilon n_{2,1} = 2.32$ π mm-mr

Normalized longitudinal momentum spread at final focus

$\delta pp_{2,1} := \delta p_p(Tf_2, \Delta Tpar_{2,1}, A_2, C_{dr})$ $\delta pp_{2,1} = 1.9 \cdot 10^{-4}$ (delta p/p)

Best final focusing angle

$\theta f_{2,1} := \theta_f(Tf_2, 4 \cdot \Delta T_{perp}, \Delta Tpar_{2,1}, A_2, as_{2,1}, L_f, C_{dr})$ $\theta f_{2,1} \cdot 10^3 = 27$ (mrad)

Minimum spot radius on target

$rsm_{2,1} := r_{sm}(Tf_2, 4 \cdot \Delta T_{perp}, \Delta Tpar_{2,1}, A_2, as_{2,1}, L_f, C_{dr})$ $rsm_{2,1} \cdot 10^6 = 217$ (μm)

Case 2.2: Neon-high q

Atomic mass $A_2 := 20.2$ Final ion energy for R=4g/cm^2 $Tf_2 := 2.7 \cdot 10^9$ (eV)

Final ion beta $\beta(Tf_2, A_2) = 0.48$ Final ion gamma $\gamma(Tf_2, A_2) = 1.14$

Charge state $q_{2,2} := 8$ Charge to mass ratio $q_{2,2} \cdot (A_2)^{-1} = 0.4$

Accelerator length

$La_{2,2} := L_a(Tf_2, q_{2,2}, A_2)$ $La_{2,2} = 106$ (m)

Source current per beam

$Is_{2,2} := I_s(q_{2,2}, A_2)$ $Is_{2,2} = 6.2$ (A)

Injection pulse length

$\tau o_{2,2} := \tau_o(Tf_2, q_{2,2}, A_2)$ $\tau o_{2,2} \cdot 10^9 = 345$ (ns)

Number of beams

$Nb_{2,2} := N_b(Tf_2, q_{2,2}, A_2)$ $Nb_{2,2} = 414$

Injected beam length

$Lbo_{2,2} := L_{bo}(Tf_2, q_{2,2}, A_2)$ $Lbo_{2,2} = 4.2$ (m)

Injector source radius

$as_{2,2} := a_s(Tf_2, q_{2,2}, A_2)$ $as_{2,2} = 0.013$ (m)

Beam length at end of accelerator

$Lba_{2,2} := L_{ba}(Tf_2, q_{2,2}, A_2)$ $Lba_{2,2} = 0.254$ (m)

Current/beam at end of the accelerator

$Ia_{2,2} := I_a(Tf_2, q_{2,2}, A_2)$ $Ia_{2,2} \cdot 10^{-3} = 1.23$ (kA)

"Effective" beam compression ratio in accelerator

$Car_{2,2} := C_{ar}(Tf_2, q_{2,2}, A_2)$ $Car_{2,2} = 4.1$

Number of voltage gaps @ 200 kV/gap

$Ng_{2,2} := N_g(Tf_2, q_{2,2})$ $Ng_{2,2} = 1.688 \cdot 10^3$ gaps

Parallel beam temperature at end of accelerator

$\Delta Tpar_{2,2} := \Delta T_{par}(Tf_2, Ng_{2,2}, \delta V_{Vp}, Car_{2,2})$ $\Delta Tpar_{2,2} = 2.7 \cdot 10^5$ (eV)

Transverse beam emittance 2x source emittance

$\varepsilon n_{2,2} := \varepsilon_n(Tf_2, 4 \cdot \Delta T_{perp}, A_2, as_{2,2})$ $\varepsilon n_{2,2} = 1.88$ π mm-mr

Normalized longitudinal momentum spread at final focus

$\delta pp_{2,2} := \delta p_p(Tf_2, \Delta Tpar_{2,2}, A_2, C_{dr})$ $\delta pp_{2,2} = 5.3 \cdot 10^{-4}$ (delta p/p)

Best final focusing angle

$\theta f_{2,2} := \theta_f(Tf_2, 4 \cdot \Delta T_{perp}, \Delta Tpar_{2,2}, A_2, as_{2,2}, L_f, C_{dr})$ $\theta f_{2,2} \cdot 10^3 = 15$ (mrad)

Minimum spot radius on target

$rsm_{2,2} := r_{sm}(Tf_2, 4 \cdot \Delta T_{perp}, \Delta Tpar_{2,2}, A_2, as_{2,2}, L_f, C_{dr})$ $rsm_{2,2} \cdot 10^6 = 330$ (μm)

Case 3.1: Argon-low q

Atomic mass $A_3 := 40$ Final ion energy for R=4g/cm^2 $Tf_3 := 7\cdot10^9$ (eV)

Final ion beta $\beta(Tf_3, A_3) = 0.54$ Final ion gamma $\gamma(Tf_3, A_3) = 1.19$

Charge state $q_{3,1} := 1$ Charge to mass ratio $q_{3,1}\cdot(A_3)^{-1} = 0.025$

Accelerator length

$La_{3,1} := L_a(Tf_3, q_{3,1}, A_3)$ $La_{3,1} = 1.79\cdot10^3$ (m)

Source current per beam

$Is_{3,1} := I_s(q_{3,1}, A_3)$ $Is_{3,1} = 1.6$ (A)

Injection pulse length

$\tau o_{3,1} := \tau_o(Tf_3, q_{3,1}, A_3)$ $\tau o_{3,1}\cdot10^9 = 1.7\cdot10^3$ (ns)

Number of beams

$Nb_{3,1} := N_b(Tf_3, q_{3,1}, A_3)$ $Nb_{3,1} = 16$

Injected beam length

$Lbo_{3,1} := L_{bo}(Tf_3, q_{3,1}, A_3)$ $Lbo_{3,1} = 5.3$ (m)

Injector source radius

$as_{3,1} := a_s(Tf_3, q_{3,1}, A_3)$ $as_{3,1} = 0.017$ (m)

Beam length at end of accelerator

$Lba_{3,1} := L_{ba}(Tf_3, q_{3,1}, A_3)$ $Lba_{3,1} = 0.282$ (m)

Current/beam at end of the accelerator

$Ia_{3,1} := I_a(Tf_3, q_{3,1}, A_3)$ $Ia_{3,1}\cdot10^{-3} = 1.52$ (kA)

"Effective" beam compression ratio in accelerator

$Car_{3,1} := C_{ar}(Tf_3, q_{3,1}, A_3)$ $Car_{3,1} = 4.3$

Number of voltage gaps @ 200 kV/gap

$Ng_{3,1} := N_g(Tf_3, q_{3,1})$ $Ng_{3,1} = 3.5\cdot10^4$ gaps

Parallel beam temperature at end of accelerator

$\Delta Tpar_{3,1} := \Delta T_{par}(Tf_3, Ng_{3,1}, \delta V_{Vp}, Car_{3,1})$ $\Delta Tpar_{3,1} = 1.6\cdot10^5$ (eV)

Transverse beam emittance 2x source emittance

$\varepsilon n_{3,1} := \varepsilon_n(Tf_3, 4\cdot\Delta T_{perp}, A_3, as_{3,1})$ $\varepsilon n_{3,1} = 1.91$ π mm-mr

Normalized longitudinal momentum spread at final focus

$\delta pp_{3,1} := \delta p_p(Tf_3, \Delta Tpar_{3,1}, A_3, C_{dr})$ $\delta pp_{3,1} = 1.3\cdot10^{-4}$ (delta p/p)

Best final focusing angle

$\theta f_{3,1} := \theta_f(Tf_3, 4\cdot\Delta T_{perp}, \Delta Tpar_{3,1}, A_3, as_{3,1}, L_f, C_{dr})$ $\theta f_{3,1}\cdot10^3 = 28$ (mrad)

Minimum spot radius on target

$rsm_{3,1} := r_{sm}(Tf_3, 4\cdot\Delta T_{perp}, \Delta Tpar_{3,1}, A_3, as_{3,1}, L_f, C_{dr})$ $rsm_{3,1}\cdot10^6 = 150$ (μm)

Case 3.2: Argon-high q

Atomic mass $A_3 := 40$ Final ion energy for R=4g/cm^2 $Tf_3 := 7\cdot10^9$ (eV)

Final ion beta $\beta(Tf_3, A_3) = 0.54$ Final ion gamma $\gamma(Tf_3, A_3) = 1.19$

Charge state $q_{3,2} := 16$ Charge to mass ratio $q_{3,2}\cdot(A_3)^{-1} = 0.4$

Accelerator length

$La_{3,2} := L_a(Tf_3, q_{3,2}, A_3)$ $La_{3,2} = 137$ (m)

Source current per beam

$Is_{3,2} := I_s(q_{3,2}, A_3)$ $Is_{3,2} = 6$ (A)

Injection pulse length

$\tau o_{3,2} := \tau_o(Tf_3, q_{3,2}, A_3)$ $\tau o_{3,2}\cdot10^9 = 425$ (ns)

Number of beams

$Nb_{3,2} := N_b(Tf_3, q_{3,2}, A_3)$ $Nb_{3,2} = 258$

Injected beam length

$Lbo_{3,2} := L_{bo}(Tf_3, q_{3,2}, A_3)$ $Lbo_{3,2} = 5.3$ (m)

Injector source radius

$as_{3,2} := a_s(Tf_3, q_{3,2}, A_3)$ $as_{3,2} = 0.013$ (m)

Beam length at end of accelerator

$Lba_{3,2} := L_{ba}(Tf_3, q_{3,2}, A_3)$ $Lba_{3,2} = 0.282$ (m)

Current/beam at end of the accelerator

$Ia_{3,2} := I_a(Tf_3, q_{3,2}, A_3)$ $Ia_{3,2}\cdot10^{-3} = 1.52$ (kA)

"Effective" beam compression ratio in accelerator

$Car_{3,2} := C_{ar}(Tf_3, q_{3,2}, A_3)$ $Car_{3,2} = 4.3$

Number of voltage gaps @ 200 kV/gap

$Ng_{3,2} := N_g(Tf_3, q_{3,2})$ $Ng_{3,2} = 2.188\cdot10^3$ gaps

Parallel beam temperature at end of accelerator

$\Delta Tpar_{3,2} := \Delta T_{par}(Tf_3, Ng_{3,2}, \delta V_{Vp}, Car_{3,2})$ $\Delta Tpar_{3,2} = 6.5\cdot10^5$ (eV)

Transverse beam emittance 2x source emittance

$\varepsilon n_{3,2} := \varepsilon_n(Tf_3, 4\cdot\Delta T_{perp}, A_3, as_{3,2})$ $\varepsilon n_{3,2} = 1.45$ π mm-mr

Normalized longitudinal momentum spread at final focus

$\delta pp_{3,2} := \delta p_p(Tf_3, \Delta Tpar_{3,2}, A_3, C_{dr})$ $\delta pp_{3,2} = 5\cdot10^{-4}$ (delta p/p)

Best final focusing angle

$\theta f_{3,2} := \theta_f(Tf_3, 4\cdot\Delta T_{perp}, \Delta Tpar_{3,2}, A_3, as_{3,2}, L_f, C_{dr})$ $\theta f_{3,2}\cdot10^3 = 12$ (mrad)

Minimum spot radius on target

$rsm_{3,2} := r_{sm}(Tf_3, 4\cdot\Delta T_{perp}, \Delta Tpar_{3,2}, A_3, as_{3,2}, L_f, C_{dr})$ $rsm_{3,2}\cdot10^6 = 261$ (μm)

Case 4.1: Krypton-low q

Atomic mass $A_4 := 84$ Final ion energy for R=4g/cm^2 $Tf_4 := 2.1 \cdot 10^{10}$ (eV)

Final ion beta $\beta(Tf_4, A_4) = 0.61$ Final ion gamma $\gamma(Tf_4, A_4) = 1.27$

Charge state $q_{4,1} := 1$ Charge to mass ratio $q_{4,1} \cdot (A_4)^{-1} = 0.012$

Accelerator length

$La_{4,1} := L_a(Tf_4, q_{4,1}, A_4)$ $La_{4,1} = 5.3 \cdot 10^3$ (m)

Source current per beam

$Is_{4,1} := I_s(q_{4,1}, A_4)$ $Is_{4,1} = 1.1$ (A)

Injection pulse length

$\tau o_{4,1} := \tau_o(Tf_4, q_{4,1}, A_4)$ $\tau o_{4,1} \cdot 10^9 = 3.2 \cdot 10^3$ (ns)

Number of beams

$Nb_{4,1} := N_b(Tf_4, q_{4,1}, A_4)$ $Nb_{4,1} = 4$

Injected beam length

$Lbo_{4,1} := L_{bo}(Tf_4, q_{4,1}, A_4)$ $Lbo_{4,1} = 6.8$ (m)

Injector source radius

$as_{4,1} := a_s(Tf_4, q_{4,1}, A_4)$ $as_{4,1} = 0.02$ (m)

Beam length at end of accelerator

$Lba_{4,1} := L_{ba}(Tf_4, q_{4,1}, A_4)$ $Lba_{4,1} = 0.322$ (m)

Current/beam at end of the accelerator

$Ia_{4,1} := I_a(Tf_4, q_{4,1}, A_4)$ $Ia_{4,1} \cdot 10^{-3} = 1.98$ (kA)

"Effective" beam compression ratio in accelerator

$Car_{4,1} := C_{ar}(Tf_4, q_{4,1}, A_4)$ $Car_{4,1} = 4.6$

Number of voltage gaps @ 200 kV/gap

$Ng_{4,1} := N_g(Tf_4, q_{4,1})$ $Ng_{4,1} = 1.05 \cdot 10^5$ gaps

Parallel beam temperature at end of accelerator

$\Delta Tpar_{4,1} := \Delta T_{par}(Tf_4, Ng_{4,1}, \delta V_{Vp}, Car_{4,1})$ $\Delta Tpar_{4,1} = 3 \cdot 10^5$ (eV)

Transverse beam emittance 2x source emittance

$\varepsilon n_{4,1} := \varepsilon_n(Tf_4, 4 \cdot \Delta T_{perp}, A_4, as_{4,1})$ $\varepsilon n_{4,1} = 1.6$ π mm-mr

Normalized longitudinal momentum spread at final focus

$\delta pp_{4,1} := \delta p_p(Tf_4, \Delta Tpar_{4,1}, A_4, C_{dr})$ $\delta pp_{4,1} = 7.9 \cdot 10^{-5}$ (delta p/p)

Best final focusing angle

$\theta f_{4,1} := \theta_f(Tf_4, 4 \cdot \Delta T_{perp}, \Delta Tpar_{4,1}, A_4, as_{4,1}, L_f, C_{dr})$ $\theta f_{4,1} \cdot 10^3 = 29$ (mrad)

Minimum spot radius on target

$rsm_{4,1} := r_{sm}(Tf_4, 4 \cdot \Delta T_{perp}, \Delta Tpar_{4,1}, A_4, as_{4,1}, L_f, C_{dr})$ $rsm_{4,1} \cdot 10^6 = 99$ (μm)

Case 4.2: Krypton-high q

Atomic mass $A_4 := 84$

Final ion energy for R=4g/cm^2 $Tf_4 := 2.1 \cdot 10^{10}$ (eV)

Final ion beta $\beta(Tf_4, A_4) = 0.61$

Final ion gamma $\gamma(Tf_4, A_4) = 1.27$

Charge state $q_{4,2} := 26$

Charge to mass ratio $q_{4,2} \cdot (A_4)^{-1} = 0.3$

Accelerator length

$La_{4,2} := L_a(Tf_4, q_{4,2}, A_4)$ $La_{4,2} = 242$ (m)

Source current per beam

$Is_{4,2} := I_s(q_{4,2}, A_4)$ $Is_{4,2} = 6$ (A)

Injection pulse length

$\tau o_{4,2} := \tau_o(Tf_4, q_{4,2}, A_4)$ $\tau o_{4,2} \cdot 10^9 = 628$ (ns)

Number of beams

$Nb_{4,2} := N_b(Tf_4, q_{4,2}, A_4)$ $Nb_{4,2} = 107$

Injected beam length

$Lbo_{4,2} := L_{bo}(Tf_4, q_{4,2}, A_4)$ $Lbo_{4,2} = 6.8$ (m)

Injector source radius

$as_{4,2} := a_s(Tf_4, q_{4,2}, A_4)$ $as_{4,2} = 0.014$ (m)

Beam length at end of accelerator

$Lba_{4,2} := L_{ba}(Tf_4, q_{4,2}, A_4)$ $Lba_{4,2} = 0.322$ (m)

Current/beam at end of the accelerator

$Ia_{4,2} := I_a(Tf_4, q_{4,2}, A_4)$ $Ia_{4,2} \cdot 10^{-3} = 1.98$ (kA)

"Effective" beam compression ratio in accelerator

$Car_{4,2} := C_{ar}(Tf_4, q_{4,2}, A_4)$ $Car_{4,2} = 4.6$

Number of voltage gaps @ 200 kV/gap

$Ng_{4,2} := N_g(Tf_4, q_{4,2})$ $Ng_{4,2} = 4 \cdot 10^3$ gaps

Parallel beam temperature at end of accelerator

$\Delta Tpar_{4,2} := \Delta T_{par}(Tf_4, Ng_{4,2}, \delta V_{Vp}, Car_{4,2})$ $\Delta Tpar_{4,2} = 1.5 \cdot 10^6$ (eV)

Transverse beam emittance 2x source emittance

$\varepsilon n_{4,2} := \varepsilon_n(Tf_4, 4 \cdot \Delta T_{perp}, A_4, as_{4,2})$ $\varepsilon n_{4,2} = 1.15$ π mm-mr

Normalized longitudinal momentum spread at final focus

$\delta pp_{4,2} := \delta p_p(Tf_4, \Delta Tpar_{4,2}, A_4, C_{dr})$ $\delta pp_{4,2} = 4.1 \cdot 10^{-4}$ (delta p/p)

Best final focusing angle

$\theta f_{4,2} := \theta_f(Tf_4, 4 \cdot \Delta T_{perp}, \Delta Tpar_{4,2}, A_4, as_{4,2}, L_f, C_{dr})$ $\theta f_{4,2} \cdot 10^3 = 11$ (mrad)

Minimum spot radius on target

$rsm_{4,2} := r_{sm}(Tf_4, 4 \cdot \Delta T_{perp}, \Delta Tpar_{4,2}, A_4, as_{4,2}, L_f, C_{dr})$ $rsm_{4,2} \cdot 10^6 = 190$ (μm)

Case 5.1: Xenon-low q

Atomic mass $A_5 := 131$ Final ion energy for R=4g/cm^2 $Tf_5 := 4\cdot10^{10}$ (eV)

Final ion beta $\beta(Tf_5, A_5) = 0.66$ Final ion gamma $\gamma(Tf_5, A_5) = 1.33$

Charge state $q_{5,1} := 1$ Charge to mass ratio $q_{5,1}\cdot(A_5)^{-1} = 7.634\cdot10^{-3}$

Accelerator length

$La_{5,1} := L_a(Tf_5, q_{5,1}, A_5)$ $La_{5,1} = 1.01\cdot10^4$ (m)

Source current per beam

$Is_{5,1} := I_s(q_{5,1}, A_5)$ $Is_{5,1} = 0.9$ (A)

Injection pulse length

$\tau o_{5,1} := \tau_o(Tf_5, q_{5,1}, A_5)$ $\tau o_{5,1}\cdot10^9 = 4.6\cdot10^3$ (ns)

Number of beams

$Nb_{5,1} := N_b(Tf_5, q_{5,1}, A_5)$ $Nb_{5,1} = 1.9$

Injected beam length

$Lbo_{5,1} := L_{bo}(Tf_5, q_{5,1}, A_5)$ $Lbo_{5,1} = 7.8$ (m)

Injector source radius

$as_{5,1} := a_s(Tf_5, q_{5,1}, A_5)$ $as_{5,1} = 0.021$ (m)

Beam length at end of accelerator

$Lba_{5,1} := L_{ba}(Tf_5, q_{5,1}, A_5)$ $Lba_{5,1} = 0.344$ (m)

Current/beam at end of the accelerator

$Ia_{5,1} := I_a(Tf_5, q_{5,1}, A_5)$ $Ia_{5,1}\cdot10^{-3} = 2.26$ (kA)

"Effective" beam compression ratio in accelerator

$Car_{5,1} := C_{ar}(Tf_5, q_{5,1}, A_5)$ $Car_{5,1} = 4.8$

Number of voltage gaps @ 200 kV/gap

$Ng_{5,1} := N_g(Tf_5, q_{5,1})$ $Ng_{5,1} = 2\cdot10^5$ gaps

Parallel beam temperature at end of accelerator

$\Delta Tpar_{5,1} := \Delta T_{par}(Tf_5, Ng_{5,1}, \delta V_{Vp}, Car_{5,1})$ $\Delta Tpar_{5,1} = 4.3\cdot10^5$ (eV)

Transverse beam emittance 2x source emittance

$\varepsilon n_{5,1} := \varepsilon_n(Tf_5, 4\cdot\Delta T_{perp}, A_5, as_{5,1})$ $\varepsilon n_{5,1} = 1.44$ π mm-mr

Normalized longitudinal momentum spread at final focus

$\delta pp_{5,1} := \delta p_p(Tf_5, \Delta Tpar_{5,1}, A_5, C_{dr})$ $\delta pp_{5,1} = 6.1\cdot10^{-5}$ (delta p/p)

Best final focusing angle

$\theta f_{5,1} := \theta_f(Tf_5, 4\cdot\Delta T_{perp}, \Delta Tpar_{5,1}, A_5, as_{5,1}, L_f, C_{dr})$ $\theta f_{5,1}\cdot10^3 = 30$ (mrad)

Minimum spot radius on target

$rsm_{5,1} := r_{sm}(Tf_5, 4\cdot\Delta T_{perp}, \Delta Tpar_{5,1}, A_5, as_{5,1}, L_f, C_{dr})$ $rsm_{5,1}\cdot10^6 = 78$ (μm)

Case 5.2: Xenon-high q

Atomic mass $A_5 := 131$ Final ion energy for R=4g/cm^2 $Tf_5 := 4\cdot10^{10}$ (eV)

Final ion beta $\beta(Tf_5, A_5) = 0.66$ Final ion gamma $\gamma(Tf_5, A_5) = 1.33$

Charge state $q_{5,2} := 26$ Charge to mass ratio $q_{5,2}\cdot(A_5)^{-1} = 0.2$

Accelerator length

$La_{5,2} := L_a(Tf_5, q_{5,2}, A_5)$ $La_{5,2} = 436$ (m)

Source current per beam

$Is_{5,2} := I_s(q_{5,2}, A_5)$ $Is_{5,2} = 4$ (A)

Injection pulse length

$\tau o_{5,2} := \tau_o(Tf_5, q_{5,2}, A_5)$ $\tau o_{5,2}\cdot10^9 = 897$ (ns)

Number of beams

$Nb_{5,2} := N_b(Tf_5, q_{5,2}, A_5)$ $Nb_{5,2} = 49$

Injected beam length

$Lbo_{5,2} := L_{bo}(Tf_5, q_{5,2}, A_5)$ $Lbo_{5,2} = 7.8$ (m)

Injector source radius

$as_{5,2} := a_s(Tf_5, q_{5,2}, A_5)$ $as_{5,2} = 0.015$ (m)

Beam length at end of accelerator

$Lba_{5,2} := L_{ba}(Tf_5, q_{5,2}, A_5)$ $Lba_{5,2} = 0.344$ (m)

Current/beam at end of the accelerator

$Ia_{5,2} := I_a(Tf_5, q_{5,2}, A_5)$ $Ia_{5,2}\cdot10^{-3} = 2.26$ (kA)

"Effective" beam compression ratio in accelerator

$Car_{5,2} := C_{ar}(Tf_5, q_{5,2}, A_5)$ $Car_{5,2} = 4.8$

Number of voltage gaps @ 200 kV/gap

$Ng_{5,2} := N_g(Tf_5, q_{5,2})$ $Ng_{5,2} = 7.7\cdot10^3$ gaps

Parallel beam temperature at end of accelerator

$\Delta Tpar_{5,2} := \Delta T_{par}(Tf_5, Ng_{5,2}, \delta V_{Vp}, Car_{5,2})$ $\Delta Tpar_{5,2} = 2.2\cdot10^6$ (eV)

Transverse beam emittance 2x source emittance

$\varepsilon n_{5,2} := \varepsilon_n(Tf_5, 4\cdot\Delta T_{perp}, A_5, as_{5,2})$ $\varepsilon n_{5,2} = 1.04$ π mm-mr

Normalized longitudinal momentum spread at final focus

$\delta pp_{5,2} := \delta p_p(Tf_5, \Delta Tpar_{5,2}, A_5, C_{dr})$ $\delta pp_{5,2} = 3.1\cdot10^{-4}$ (delta p/p)

Best final focusing angle

$\theta f_{5,2} := \theta_f(Tf_5, 4\cdot\Delta T_{perp}, \Delta Tpar_{5,2}, A_5, as_{5,2}, L_f, C_{dr})$ $\theta f_{5,2}\cdot10^3 = 11$ (mrad)

Minimum spot radius on target

$rsm_{5,2} := r_{sm}(Tf_5, 4\cdot\Delta T_{perp}, \Delta Tpar_{5,2}, A_5, as_{5,2}, L_f, C_{dr})$ $rsm_{5,2}\cdot10^6 = 149$ (μm)

Case 6.1: Lead-low q

Atomic mass $A_6 := 207$ Final ion energy for R=4g/cm^2 $Tf_6 := 9 \cdot 10^{10}$ (eV)

Final ion beta $\beta(Tf_6, A_6) = 0.73$ Final ion gamma $\gamma(Tf_6, A_6) = 1.46$

Charge state $q_{6,1} := 1$ Charge to mass ratio $q_{6,1} \cdot (A_6)^{-1} = 4.831 \cdot 10^{-3}$

Accelerator length

$La_{6,1} := L_a(Tf_6, q_{6,1}, A_6)$ $La_{6,1} = 2.26 \cdot 10^4$ (m)

Source current per beam

$Is_{6,1} := I_s(q_{6,1}, A_6)$ $Is_{6,1} = 0.7$ (A)

Injection pulse length

$\tau o_{6,1} := \tau_o(Tf_6, q_{6,1}, A_6)$ $\tau o_{6,1} \cdot 10^9 = 7.1 \cdot 10^3$ (ns)

Number of beams

$Nb_{6,1} := N_b(Tf_6, q_{6,1}, A_6)$ $Nb_{6,1} = 0.7$

Injected beam length

$Lbo_{6,1} := L_{bo}(Tf_6, q_{6,1}, A_6)$ $Lbo_{6,1} = 9.7$ (m)

Injector source radius

$as_{6,1} := a_s(Tf_6, q_{6,1}, A_6)$ $as_{6,1} = 0.023$ (m)

Beam length at end of accelerator

$Lba_{6,1} := L_{ba}(Tf_6, q_{6,1}, A_6)$ $Lba_{6,1} = 0.383$ (m)

Current/beam at end of the accelerator

$Ia_{6,1} := I_a(Tf_6, q_{6,1}, A_6)$ $Ia_{6,1} \cdot 10^{-3} = 2.8$ (kA)

"Effective" beam compression ratio in accelerator

$Car_{6,1} := C_{ar}(Tf_6, q_{6,1}, A_6)$ $Car_{6,1} = 5$

Number of voltage gaps @ 200 kV/gap

$Ng_{6,1} := N_g(Tf_6, q_{6,1})$ $Ng_{6,1} = 4.5 \cdot 10^5$ gaps

Parallel beam temperature at end of accelerator

$\Delta Tpar_{6,1} := \Delta T_{par}(Tf_6, Ng_{6,1}, \delta V_{Vp}, Car_{6,1})$ $\Delta Tpar_{6,1} = 6.7 \cdot 10^5$ (eV)

Transverse beam emittance 2x source emittance

$\varepsilon n_{6,1} := \varepsilon_n(Tf_6, 4 \cdot \Delta T_{perp}, A_6, as_{6,1})$ $\varepsilon n_{6,1} = 1.38$ π mm-mr

Normalized longitudinal momentum spread at final focus

$\delta pp_{6,1} := \delta p_p(Tf_6, \Delta Tpar_{6,1}, A_6, C_{dr})$ $\delta pp_{6,1} = 4.5 \cdot 10^{-5}$ (delta p/p)

Best final focusing angle

$\theta f_{6,1} := \theta_f(Tf_6, 4 \cdot \Delta T_{perp}, \Delta Tpar_{6,1}, A_6, as_{6,1}, L_f, C_{dr})$ $\theta f_{6,1} \cdot 10^3 = 31$ (mrad)

Minimum spot radius on target

$rsm_{6,1} := r_{sm}(Tf_6, 4 \cdot \Delta T_{perp}, \Delta Tpar_{6,1}, A_6, as_{6,1}, L_f, C_{dr})$ $rsm_{6,1} \cdot 10^6 = 59$ (μm)

Case 6.1: Lead-high q

Atomic mass $A_6 := 207$ Final ion energy for R=4g/cm² $Tf_6 := 9 \cdot 10^{10}$ (eV)

Final ion beta $\beta(Tf_6, A_6) = 0.73$ Final ion gamma $\gamma(Tf_6, A_6) = 1.46$

Charge state $q_{6,2} := 49$ Charge to mass ratio $q_{6,2} \cdot (A_6)^{-1} = 0.237$

Accelerator length

$La_{6,2} := L_a(Tf_6, q_{6,2}, A_6)$ $La_{6,2} = 525$ (m)

Source current per beam

$Is_{6,2} := I_s(q_{6,2}, A_6)$ $Is_{6,2} = 4.8$ (A)

Injection pulse length

$\tau o_{6,2} := \tau_o(Tf_6, q_{6,2}, A_6)$ $\tau o_{6,2} \cdot 10^9 = 1.02 \cdot 10^3$ (ns)

Number of beams

$Nb_{6,2} := N_b(Tf_6, q_{6,2}, A_6)$ $Nb_{6,2} = 33.3$

Injected beam length

$Lbo_{6,2} := L_{bo}(Tf_6, q_{6,2}, A_6)$ $Lbo_{6,2} = 9.7$ (m)

Injector source radius

$as_{6,2} := a_s(Tf_6, q_{6,2}, A_6)$ $as_{6,2} = 0.016$ (m)

Beam length at end of accelerator

$Lba_{6,2} := L_{ba}(Tf_6, q_{6,2}, A_6)$ $Lba_{6,2} = 0.383$ (m)

Current/beam at end of the accelerator

$Ia_{6,2} := I_a(Tf_6, q_{6,2}, A_6)$ $Ia_{6,2} \cdot 10^{-3} = 2.8$ (kA)

"Effective" beam compression ratio in accelerator

$Car_{6,2} := C_{ar}(Tf_6, q_{6,2}, A_6)$ $Car_{6,2} = 5$

Number of voltage gaps @ 200 kV/gap

$Ng_{6,2} := N_g(Tf_6, q_{6,2})$ $Ng_{6,2} = 9.184 \cdot 10^3$ gaps

Parallel beam temperature at end of accelerator

$\Delta Tpar_{6,2} := \Delta T_{par}(Tf_6, Ng_{6,2}, \delta V_{Vp}, Car_{6,2})$ $\Delta Tpar_{6,2} = 4.7 \cdot 10^6$ (eV)

Transverse beam emittance 2x source emittance

$\varepsilon n_{6,2} := \varepsilon_n(Tf_6, 4 \cdot \Delta T_{perp}, A_6, as_{6,2})$ $\varepsilon n_{6,2} = 0.93$ π mm-mr

Normalized longitudinal momentum spread at final focus

$\delta pp_{6,2} := \delta p_p(Tf_6, \Delta Tpar_{6,2}, A_6, C_{dr})$ $\delta pp_{6,2} = 3.1 \cdot 10^{-4}$ (delta p/p)

Best final focusing angle

$\theta f_{6,2} := \theta_f(Tf_6, 4 \cdot \Delta T_{perp}, \Delta Tpar_{6,2}, A_6, as_{6,2}, L_f, C_{dr})$ $\theta f_{6,2} \cdot 10^3 = 10$ (mrad)

Minimum spot radius on target

$rsm_{6,2} := r_{sm}(Tf_6, 4 \cdot \Delta T_{perp}, \Delta Tpar_{6,2}, A_6, as_{6,2}, L_f, C_{dr})$ $rsm_{6,2} \cdot 10^6 = 128$ (μm)

IV. Summary of results, required core volumes, power switching, transport

Table 1 Summary of results of the survey of different masses and charge states for fast ignition.

Common assumptions/constraints: Total ion energy for ignition = 300 kJ, ion range = 4 g/cm2, source ion temperature 20 eV, emittance doubling during acceleration, injector voltage = 2 MV, maximum acceleration gradient 4 MV/m, maximum longitudinal space-charge E_z <1.2 MV/m at end of accelerator, 0.1% pulser voltage regulation, space charge neutralized to better than 99.5 % during 10x drift compression and chamber transport, 0.5% velocity tilt aberration corrected by 7 kA/ns e-beam injection after focus, beam pulse at focus = 175 ps, at target =50 ps. Spot radius is calculated for each case [the target requirement is r_s < 156μm]

For $j := 1..6$ different ion masses, and for $k := 1..2$ charge states for each ion

Species	Mass A_j	Ion energy $Tf_j / 10^9$	Low charge $q_{j,1}$	Accel length $La_{j,1}$	# of beams $Nb_{j,1}$	focus angle $\theta f_{j,1} / 10^{-3}$	spot radius $rsm_{j,1} / 10^{-6}$	High charge $q_{j,2}$	Accel length $La_{j,2}$	# of beams $Nb_{j,2}$	focus angle $\theta f_{j,2} / 10^{-3}$	spot radius $rsm_{j,2} / 10^{-6}$
Helium	4	0.22	1	64	1379	25	563	2	35	2757	21	647
Neon	20.2	2.7	1	705	52	27	217	8	106	414	15	330
Argon	40	7	1	1792	16	28	150	16	137	258	12	261
Krypton	84	21	1	5313	4	29	99	26	242	107	11	190
Xenon	131	40	1	10078	2	30	78	26	436	49	11	149
Lead	207	90	1	22604	1	31	59	49	525	33	10	128
	(amu)	(GeV)		(m)		(mr)	(μm)		(m)		(mr)	(μm)

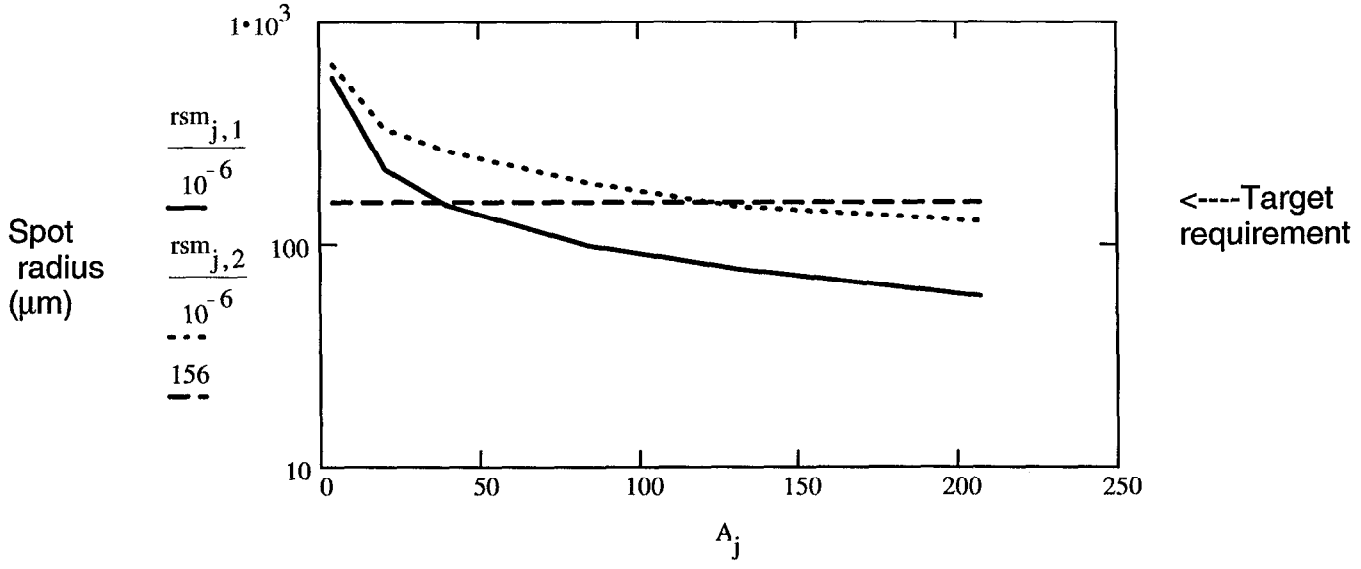

Figure 5: Comparison of minimum beam spot radii (r_{sm} in microns) versus ion mass, for q=1 ions (solid red line), and for high charge states (dotted blue line) -seeTable 1 for q values.

From Fig. 5 one concludes heavier ions are best to achieve fast ignition. Compare ion cases at nearly the same charge-to-mass ratio as Helium^{+1} (q/A =0.25) : Lead^{+49} (q/A=0.24), and Xenon^{+26} (q/A=0.2), can achieve four times smaller spot sizes under the above model and constraints. At any given mass the smallest spot size is still achieved at the minimum q=1, but the spot size is only a factor of two lower. As long as the spot size is smaller than the target requirement, one can raise the q to reduce the accelerator length and cost. The highest q heavy ion cases meet the spot size requirement but also reduce the length of the accelerator by large factors of q. Thus, if one wants to meet the stringent spot size required for fast ignition as well as keep the accelerator cost low (to reap a net benefit from fast ignition), one wants both the highest q and highest mass ions. Much of the benefit from heavy-ions comes from the higher $\beta\gamma$ for a given ion range. Lead has almost 3 times higher $\beta\gamma$ than helium for the same range. The higher $\beta\gamma$ helps both in management of space charge (see the $(\beta\gamma)^3$ factor in Eq. 3 for the required neutralization fraction, (which is derived from the envelope equation), and for a given absolut ΔT_{par} longitudinal energy spread, the relativistic $\delta p/p$ has a $\beta^2\gamma$ in the denominator of Eq. 5. The following physical parameters for major accelerator subsystems are estimated for our reference case Xe+26 (40 GeV).

Transport

The maximum transportable current for a quadrupole FODO lattice is given by

$$I_{trans}(B_q, a_b, T, A, \eta_q) := 8\cdot 10^5 \cdot B_q \cdot a_b \cdot \beta(T,A)^2 \cdot \gamma(T,A)^2 \cdot \eta_q \qquad \text{Eq.24}$$

Lets take Tf/3 to be a representative ion energy point for the linac with a ramped acceleration gradient as shown in Fig. 1. For the Xe^{+26} case, the beam current there is

$$I_s(26,131)\cdot\beta\left(0.33\cdot 40\cdot 10^9, 131\right)^2 \cdot \beta\left(26\cdot V_s, 131\right)^{-2} = 962.9 \quad \text{Amps}$$

Setting the transportable current (Eq. 24) to the beam current at that point, we can solve for a required average quad occupancy fraction η_q :

$$\eta_q(T_f, q, A, B_q, a_b) := \frac{I_s(q,A)\cdot\beta\left(0.33\cdot T_f, A\right)^2 \cdot \beta\left(q\cdot V_s, A\right)^{-2}}{8\cdot 10^5 \cdot B_q \cdot a_b \cdot \beta\left(0.33\cdot T_f, A\right)^2 \cdot \gamma\left(0.33\cdot T_f, A\right)^2} \qquad \text{Eq.25}$$

For our reference Xe^{+26} case, taking a quadrupole field (at bore) $B_q := 3$ (T)

and at a beam radius $a_b := 0.02$ (m)

Eq. 25 gives $\eta_q\left(40\cdot 10^9, 26, 131, B_q, a_b\right) = 0.09$

For an average quad length = 50 cm, there would be a quad every 5.5 meters! [Another nice consequence of having a high $\beta\gamma$!] The total number of quads for our reference fast ignitor linac case would be

$$\frac{La_{5,2}\cdot Nb_{5,2}}{5.5} = 3.9\cdot 10^3$$

quads. For reference, the Heidelberg baseline design for a conventional HIF target requiring 5.9 MJ delivered in 48 beams requires *120 thousand* magnetic quads of similar field and size.

Cores

Metglas

For our reference Xe+26 case with initial beam duration $\tau o_{5,2} = 9 \cdot 10^{-7}$ sec

One would use metglas cores from this pulse length to the ion energy point at which the beam pulse length would be one tenth of this:

$$T := 10 \cdot 26 \cdot V_s \qquad T = 5.2 \cdot 10^8$$

$$T_c(q,A) := \text{root}\left[\left(\frac{\beta(T,A)}{\beta\left(q \cdot V_s, A\right)}\right)^2 - 10, T\right] \qquad T_c(26,131) = 5.23 \cdot 10^8 \text{ (eV)} \qquad \text{Eq. 26}$$

The length of this section of the accelerator which would use metglas is

$$L_{met}\left(T_f, q, A\right) := \int_{q \cdot V_s}^{T_c(q,A)} \frac{1 + T \cdot \left[q \cdot \left(\tau_o\left(T_f, q, A\right) \cdot \beta\left(q \cdot V_s, A\right) \cdot c\right)\right]^{-1} \cdot V_{gm}^{-1}}{T \cdot \left[q \cdot \left(\tau_o\left(T_f, q, A\right) \cdot \beta\left(q \cdot V_s, A\right) \cdot c\right)\right]^{-1} \cdot q} dT \qquad \text{Eq. 27}$$

$$L_{met}\left(40 \cdot 10^9, 26, 131\right) = 23 \qquad \text{(m)}$$

The outer quad radius is $a_q\left(a_b, B_q\right) := 1.25 \cdot a_b + 10^{-2} \cdot \left(1 + 0.2 \cdot B_q\right)$ (m)

$$a_q\left(a_b, B_q\right) = 0.041$$

leading to an inner core radius R_c for cores that would surround all N_b =50 beams:

$$R_c\left(a_q, N_b\right) := a_q \cdot \sqrt{\frac{N_b}{0.65}} + 0.05 \qquad \text{Eq. 28}$$

$$R_c\left(a_q\left(a_b, B_q\right), Nb_{5,2}\right) = 0.407 \qquad \text{(m)}$$

The radial build of the metglas cores is estimated by

$$\Delta R_c\left(V_g, \tau, \Delta B_c\right) := \frac{V_g \cdot \tau}{0.64 \cdot \Delta B_c} \qquad \text{(m)} \qquad \text{Eq. 29}$$

where 0.64 accounts for 0.8x0.8 packing fractions, and $\Delta B_{met} := 2$ (T) flux swing for metglas

The induction pulse τ scales with, but is in general longer than, the beam pulse width at any point.

At the injector $\Delta R_c\left(V_g\left(26\cdot V_s, 26, Lbo_{5,2}\right), 1.1\cdot \tau o_{5,2}, \Delta B_{met}\right) = 0.185$ (m)

Very moderate radial build where $V_g\left(26\cdot V_s, 26, Lbo_{5,2}\right) = 2.403\cdot 10^5$ (V/m)

(the pulse length here is only 0.9 μs instead of the usual 20 μs in conventional HIF designs)

At the transition point to ferrite at $T_c(26,131) = 5.23\cdot 10^8$ (eV)

$$\Delta R_c\left(V_g\left(T_c(26,131), 26, Lbo_{5,2}\right), 1.1\cdot \frac{\tau o_{5,2}}{10}, \Delta B_{met}\right) = 0.121 \quad \text{(m)}$$

where $V_g\left(T_c(26,131), 26, Lbo_{5,2}\right) = 1.565\cdot 10^6$ (V/m).

The radial build for metglas is very modest (12 cm) at this transition point.

The total volume of cores in the metglas section from injection to the transition to ferrite is

$$V_c\left(T_c, q, A, L_{bo}, \tau, \Delta B, R_c\right) := \pi\cdot \int_{q\cdot V_s}^{T_c} \frac{2\cdot \Delta R_c\left(V_g\left(T, q, L_{bo}\right), \tau\cdot \frac{\beta\left(q\cdot V_s, A\right)^2}{\beta(T,A)^2}, \Delta B\right)\cdot R_c \ldots + \Delta R_c\left(V_g\left(T, q, L_{bo}\right), \tau\cdot \frac{\beta\left(q\cdot V_s, A\right)^2}{\beta(T,A)^2}, \Delta B\right)^2}{q\cdot V_g\left(T, q, L_{bo}\right)} dT$$

(m³) Eq. 30

$$V_c\left(T_c(26,131), 26, 131, Lbo_{5,2}, 1.1\cdot \tau o_{5,2}, \Delta B_{met}, R_c\left(a_q\left(a_b, B_q\right), Nb_{5,2}\right)\right) = 10.9 \quad (m^3)$$

The mass of metglas cores is $M_c\left(V_c\right) := 0.64\cdot 7800\cdot V_c$ (kg) Eq. 31

$$M_c\left(V_c\left(T_c(26,131), 26, 131, Lbo_{5,2}, 1.1\cdot \tau o_{5,2}, \Delta B_{met}, R_c\left(a_q\left(a_b, B_q\right), Nb_{5,2}\right)\right)\right) = 5.4\cdot 10^4 \quad (kg)$$

Ferrite (in external voltage adder configuration as shown in Fig. 2)

Since the ferrite cores for induction are supplied through external voltage adder modules, (se Fig. 2), the inner core radius is just enough for the center rod and insulation space, say

$$R_{cf} := 0.04 \qquad \text{(m)}$$

Ferrite has a smaller saturation for useful flux swing $\Delta B_{fer} := 0.5$ (T)

The radial build for ferrite at the transition energy is, taking into account that the gradient along the voltage adder is assumed to be one-fourth of the local average acceleration gradient at the beam is

$$\Delta R_c\left(\frac{V_g\left(T_c(26,131),26,Lbo_{5,2}\right)}{4}, 1.1\cdot\frac{\tau o_{5,2}}{10}, \Delta B_{fer}\right) = 0.121 \qquad \text{(m)}$$

again the local gradient at this transition is

$$V_g\left(T_c(26,131),26,Lbo_{5,2}\right) = 1.6\cdot 10^6 \qquad \text{(V/m) for the beam}$$

and

$$\frac{V_g\left(T_c(26,131),26,Lbo_{5,2}\right)}{4} = 3.9\cdot 10^5 \qquad \text{(V/m) along the voltage adders}$$

which exactly compensates for the 4 x lower flux swing for ferrite. The pulse length at this transition point is

$$1.1\cdot\frac{\tau o_{5,2}}{10} = 9.9\cdot 10^{-8} \qquad \text{(sec)}$$

The ferrite radial buid is much less at the high energy end of the linac despite the local gradient being more than 2 x higher at the end, and despite the fact that we allow for the induction pulse to grow longer than the beam pulse by a factor of 3.3 towards the high end (see Fig. 2):

$$\Delta R_c\left(\frac{V_g\left(Tf_5,26,Lbo_{5,2}\right)}{4}, 3.3\cdot 1.75\cdot 10^{-9}, \Delta B_{fer}\right) = 0.018 \qquad \text{(m)}$$

A scaling to use for the induction pulse length in volt-second calculations along the accelerator, starting from some point τ, is

$$\tau_p\left(T,T_f,q,A,\tau\right) := \tau\cdot\left(\frac{\beta\left(T_c(q,A),A\right)}{\beta(T,A)}\right)^2\cdot\left(1+2\cdot\frac{T-T_c(q,A)}{T_f-T_c(q,A)}\right) \qquad \text{(s)} \qquad \text{Eq. 32}$$

Thus $$\tau_p\left(T_c(26,131),Tf_5,26,131,1.1\cdot\frac{\tau o_{5,2}}{10}\right) = 9.9\cdot 10^{-8} \qquad \text{(s)}$$

and $$\tau_p\left(Tf_5,Tf_5,26,131,1.1\cdot\frac{\tau o_{5,2}}{10}\right) = 5.8\cdot 10^{-9} \qquad \text{(s)}$$

With the above scaling for the induction pulse relative to the beam pulse, the expression for the total ferrite core volume integrated from the transition energy to the final energy is given by

$$V_f(T_c,T_f,q,A,L_{bo},\tau,\Delta B,R_c) := \pi \cdot \int_{T_c}^{T_f} \frac{\left[2\cdot\Delta R_c\left[\frac{V_g(T,q,L_{bo})}{4},\frac{\tau\cdot\frac{\beta(T_c,A)^2}{\beta(T,A)^2}}{\left(1+2\cdot\frac{T-T_c}{T_f-T_c}\right)^{-1}},\Delta B\right]\cdot R_c + \ldots \right.}{q\cdot\frac{V_g(T,q,L_{bo})}{4}} \ldots$$

$$\ldots \frac{\left. +\Delta R_c\left[\frac{V_g(T,q,L_{bo})}{4},\frac{\tau\cdot\frac{\beta(T_c,A)^2}{\beta(T,A)^2}}{\left(1+2\cdot\frac{T-T_c}{T_f-T_c}\right)^{-1}},\Delta B\right]^2\right]}{q\cdot\frac{V_g(T,q,L_{bo})}{4}} dT$$

Thus, the total volume of ferrite in the voltage adders is (m³) Eq. 33

$$V_f\left(T_c(26,131),Tf_5,26,131,Lbo_{5,2},1.1\cdot\frac{\tau o_{5,2}}{10},\Delta B_{fer},R_{cf}\right) = 16.6 \quad (m^3)$$

And the mass of the ferrite cores $M_f(V_f) := 5200\cdot V_f$ (kg) Eq. 34

$$M_f\left(V_f\left(T_c(26,131),Tf_5,26,131,Lbo_{5,2},1.1\cdot\frac{\tau o_{5,2}}{10},\Delta B_{fer},R_{cf}\right)\right) = 8.63\cdot10^4 \quad (kg)$$

Summary of core material

Total mass of metglas

$$M_c\left(V_c\left(T_c(26,131),26,131,Lbo_{5,2},1.1\cdot\tau o_{5,2},\Delta B_{met},R_c\left(a_q\left(a_b,B_q\right),Nb_{5,2}\right)\right)\right) = 5.4\cdot10^4 \quad (kg)$$

Total mass of ferrite

$$M_f\left(V_f\left(T_c(26,131),Tf_5,26,131,Lbo_{5,2},1.1\cdot\frac{\tau o_{5,2}}{10},\Delta B_{fer},R_{cf}\right)\right) = 8.63\cdot10^4 \quad (kg)$$

For reference, the total mass of metglas in the Heidelberg baseline linac for the conventional target was ~ 3×10^7 kg, or 30,000 tons! Thus, this fast ignitor linac example has **200** times less total mass of core material than the baseline linac. Ferrite is more expensive than metglas, but it also has lower losses than metglas for the same pulse lengths. More detailed study is needed to determine the ferrite losses at the very short pulses considered here.

Switching and energy storage

Very roughly, lets suppose this fast ignitor linac, mostly ferrite at short pulses, has losses per unit ferrite volume = 4 x worse than for metglas at typical conventional HIF pulse lengths, which was 10 MJ / 4000 m^3 = 2.5 kJ / m^3 for the Heidelberg baseline (average); i.e., lets assume the losses are as bad as 10 kJ / m^3 of ferrite. This means total ferrite losses in this case would be

$$\frac{8.63\cdot 10^4}{5200}\cdot 10^4 = 1.66\cdot 10^5$$ J, i.e, the efficiency would be $$\frac{3\cdot 10^5}{3\cdot 10^5 + 1.66\cdot 10^5} = 0.644$$

here, which is not counting losses in switching and pulse compression, if needed, to drive the ferrite cores at short pulses. If switching losses equaled such ferrite losses, the overall accelerator efficiency would still be a respectable 50%. This may seem surprising, until one realizes that there is 50 beams x 2.3 kA/ beam = 115 kA total beam current at the high energy end of the accelerator.

In the Heidelberg baseline, taking the avergae characteristic switching time to be~ 3 times the output pulse length of 100 ns, the total power switching was of order

$$\frac{15\cdot 10^6}{300\cdot 10^{-9}} = 5\cdot 10^{13}$$ (Watts). For an assumed cost of 300 $ per 100 MW, for thyratrons, this system was estimated to cost $150 M direct capital. In addition, the energy storage was estimated to cost $10/J, so another $150 M for energy storage, or $300M for 15 MJ, ~ $20/Joule for the pulser system.

For this fast ignitor linac example, *if the ferrite cores are directly switched with FET's*, the corresponding numbers are

$$\frac{3\cdot 10^5\cdot 0.5^{-1}}{3\cdot 5.8\cdot 10^{-9}} = 3.4\cdot 10^{13}$$ (Watts), which would be $100 M for switching if one assumed the costs were the same for FET's (extrapolated to future costs) as Thyratrons today. The energy storage costs would be only $6M @10$/Joule, because of the smaller energy storage requirement.

Because at present FET switching is still more expensive per peak watt than with Thyratrons, there is a potential cost exposure if the cost of FET's don't continue to drop in the future as they have been doing. For this reason, it may be a prudent choice to use one or two stages of magnetic pulse compression (a la ETA-II, except using ferrite instead of metglas for shorter pulses), so that the FET's are switching comparable pulse energies over 10 to 100 times longer time scales (e.g, 50 to 500 ns instead of 5 ns). This would greatly lower the cost of FET switches on the front end of such compressors, at the expense of adding additional ferrite cores for the compression stages. However, as seen above, there is not that much ferrite, so doubling or tripling the total ferrite volume with one or two stages of magnetic pulse compression, respectively, may be a better trade for lower overall costs.

Postscript: As this memo was going to press, George Caporaso, Steve Sampayan, and Hugh Kirbie informed me they are looking at the possibility of using a Dielectric Wall Accelerator (DWA) at ~ 20 MV/m acceleration gradient, for this fast ignition application. If a practical solution can be found for repeated switching of the outer circumferential surface of the dielectric lines at 5 Hz, then the accelerator examples described here would shrink in length by another factor of 5. The beam transport and focusing calculations and ordering of spot sizes with ion mass and charge state estimates here would presumably apply also to their DWA concept.

Technical Information Department • **Lawrence Livermore National Laboratory**
University of California • Livermore, California 94551